

Generalized quasi, Ioffe-time, and pseudo quark distributions of the pion in the Nambu–Jona-Lasinio model

Vanamali Shastry,^{1,*} Wojciech Broniowski,^{2,1,†} and Enrique Ruiz Arriola^{3,‡}

¹*Institute of Physics, Jan Kochanowski University, 25-406 Kielce, Poland*

²*H. Niewodniczański Institute of Nuclear Physics PAN, 31-342 Cracow, Poland*

³*Departamento de Física Atómica, Molecular y Nuclear and Instituto Carlos I de Física Teórica y Computacional, Universidad de Granada, E-18071 Granada, Spain*

(Dated: 7 September 2022)

We analyze the generalized quasi, Ioffe-time, and pseudo distributions of the valence quarks in the pion at the quark model scale. We use the framework of the Nambu–Jona-Lasinio model and investigate the basic question of how fast the pion has to move to effectively reach the infinite momentum limit, where the approach can provide the information on the generalized parton distribution functions. We consider both the vector distributions and the transversity distributions, related to the spin densities. With the developed analytic expressions, we conclude that to effectively approach the infinite momentum limit in the Ioffe-time distributions for values of the Ioffe-time accessible in lattice QCD, one roughly needs the pion momenta of the order of ~ 3 GeV. We explore polynomiality of the quasi distributions and study the generalized quasi form factors. The issue of separability of the transverse and longitudinal dynamics in the model is studied with the help of the generalized Ioffe-time distributions, with the conclusion that the breaking is not substantial, unless the momentum transfer t is large. We also provide an estimate of the range of the Ioffe-time values needed to obtain the generalized parton distributions with a reasonable accuracy. Our model results, which are analytic or semi-analytic, provide a valuable insight into the theoretical formalism and illustrate the intricate features of the investigated distributions.

I. INTRODUCTION

In recent years a significant progress has been made to directly access partonic distribution functions (PDFs) of hadrons on the Euclidean lattices. The novel techniques involve the quasi-distributions proposed by Ji [1–10] amended with the large mass effective theory (LaMET) [11–14], the pseudo-distributions [15–27], the “good lattice cross sections” method [28, 29], or the Compton Feynman–Hellman approach [30]. These methods have an ambition to reach way further than the lattice QCD determinations of the lowest Bjorken x -moments of the hadronic PDFs [31–34] and obtain the distributions as functions of the parton momentum fraction x (x is the momentum fraction of the hadron carried by the parton). The quasi distribution amplitude (qDA) of the pion on the lattice has recently been analyzed in [35]. For detailed reviews of the progress and the challenges, both for the nucleon and for mesons, see [36–40]. One should remark here that apart from the above listed methods, the valence PDF and the distribution amplitude (DA) of the pion have also been determined directly within the Hamiltonian transverse lattice approach which faces the problem in the Minkowski space [41–43].

Model determinations of the quasi parton distributions of the pion have been made in the framework of the Nambu–Jona-Lasinio (NJL) model (for a review of NJL in the context of high-energy processes see [44])

in [45, 46], with an extension to the Ioffe-time distributions (ITDs) [16, 47] provided in [48]. An analysis within a QCD instanton vacuum model has been carried out in [49].

For the nucleon, a study in a diquark spectator model was carried out in [50], a factorization ansatz was used in [46], a large- N_c model was explored in [51, 52], and the quark quasi Sivers and quasi Boer–Mulders functions were considered in [53].

On the experimental side, the current and indirect knowledge of the pion’s valence PDF originates from scattering of secondary pion beams on nuclear targets at the CERN NA3 experiment [54] and the Fermilab E615 experiment [55], as well as from the electroproduction HERA data [56, 57]. A recent global analysis has been presented in [58]. The future COMPASS++/AMBER facility at CERN, with direct pion beams, will provide separate information on the valence and sea pion PDFs, as well as on the gluon distribution, using the J/ψ and ψ' production [59]. Hence, there emerges a renewed demand for theoretical and model predictions.

An evaluation of the pion PDFs in NJL, keeping track of relativity, gauge invariance, a proper support in the Bjorken variable x , induced normalization constraints, and supplemented with the QCD evolution, was first made in [60, 61] thanks to a scrupulous implementation of a suitable regularization method. Analyses in non-local chiral quark models were provided in [62–64]. For the results of the Dyson–Schwinger approach with the rainbow ladder truncation, see [65, 66].

Extensions of PDFs to non-forward processes [67–69] are provided by the generalized parton distribution functions (GPDs) [70, 71], where the momenta of the initial

* vshastry@ujk.edu.pl

† Wojciech.Broniowski@ifj.edu.pl

‡ earriola@ugr.es

and final hadron can be different. Naturally, this enriches the insight into the hadron structure, leading to partonic tomography revealing the spatial distribution of partons in the plane transverse to the direction of motion of the hadron [72–75]. For extensive reviews of GPDs see, e.g. [76–87], where also the significance of GPDs to physical processes, such as deeply virtual Compton scattering (DVCS) or the hard meson production (HMP) is reported.

The pion GPDs in a non-local chiral quark model were presented in [88], whereas the NJL results can be found in [89–93]. In particular, analytic expressions at the quark model scale were presented in [90]. For an evaluation of the GPDs of light mesons in the light-front Hamiltonian approach see [94]. The ρ meson GPD in the NJL model was shown in [95]. Transverse lattice calculations were given in [96], with the results reproduced by an NJL calculation [97].

Recently, the accessibility of the pion GPD through the Sullivan process [98] has been brought up in the context of the future Electron-Ion Collider experiments [99, 100].

A path to obtain GPDs on the Euclidean lattice from the quasi GPDs (qGPDs) has been proposed in [101, 102], and an alternative approach based on the pseudo GPDs (pGPDs) has been advocated in [103]. In a quark spectator model, qGPDs were addressed in [104–106], whereas the first lattice-QCD results for zero-skewness GPDs were reported in [107, 108]. The limit of large- N_c in ITDs of the pion was studied in [109].

The role of model studies of quasi-distributions is based not only on the fact that they are the core of lattice studies of partonic distribution. These quantities are interesting per se as properties of hadrons related to matrix elements of bilocal operators. They also shed light on the rather intricate formalism of partonic distributions, providing nontrivial examples. This is very much so in the case of the pion which arises as the would-be Goldstone boson of the spontaneously broken chiral symmetry.

In this work we study the qGPDs and pGPDs, as well as the generalized Ioffe-time distributions of the pion in the framework of the NJL model at the low quark model scale, where the chiral symmetry features of QCD are properly implemented and expected to largely dominate the results. We also consider the transversity distributions, related to the spin distributions. With the obtained analytic or semi-analytic expressions we study the limit of the large momentum P_z of the pion, i.e., we investigate the approach of the quasi distributions to the standard GPD case. The question is of practical importance for the scheme to work, as on the lattice the upper value of P_z is naturally limited with the inverse lattice spacing, $a \sim 1/P_z$, which presently reaches (in physical units) up to about $a \sim 0.05 - 0.10$ fm and, consequently, $P_z \sim 2 - 4$ GeV only. We stress that our model approach satisfies all the general field-theoretic requirements, such as the Lorentz covariance, the gauge invariance, or crossing symmetry.

In this paper we restrict to the model results at the

quark model scale [90], and do not carry out the QCD evolution to higher scales. We are interested in exploring the $P_z \rightarrow \infty$ limit, which is generally not affected by the evolution in the sense that the discrepancy between a finite P_z and the infinite limit at the quark model scale would be carried over with the evolution to higher scales. We note that a working scheme for the evolution of qGPD, proceeding via evolution of the k_T -unintegrated distributions [110–113], has been used in [46]. Such studies for the present case, needed to compare the model results to the lattice data obtained at much higher scales, are left for a future work.

We find that to obtain reasonable GPDs, in particular the non-forward ones, requires large values of P_z , at least of the order of ~ 3 GeV. We also explore polynomiality of the quasi distributions and study in some detail the generalized quasi form factors. The issue of separability of the transverse and longitudinal dynamics in the model is studied with the help of the generalized Ioffe-time distributions

The paper is organized as follows: In Section II we review and extend the general formalism of quasi GPDs of the pion, discussing in particular the feature of polynomiality and the generalized quasi form factors, the generalized Ioffe-time distributions, and the generalized pseudo-distributions, with their relation to the k_T -unintegrated GPDs. Section III is devoted to our model results. We first briefly review the NJL model and then present its numerous analytic or semi-analytic results for the quasi distributions and related quantities introduced earlier. The proximity of the results obtained at a large but finite P_z to the $P_z \rightarrow \infty$ limit is assessed. We present the generalized Ioffe-time distributions and the generalized pseudo-distributions and discuss the issue of the separability of the longitudinal and transverse dynamics. We also elucidate the range in the Ioffe time needed to reliably pass to the x space. The Appendices contain some more technical but nevertheless useful and relevant results, such as explicit realizations of various possible kinematics for the quasi-distributions, the derivation and explicit forms of the one-loop expressions for the NJL model, or an explicit check of polynomiality for the quasi distributions.

II. BASICS

Given the large number of variables and their Fourier conjugates involved in the GPDs and related objects, there is some inherent degree of complexity which cannot be avoided. In this Section we provide a concise glossary of the necessary definitions and establish the notation of our paper. The mentioned results are general, independent of the model used later on.

A. Definitions

The valence quark GPDs and qGPDs of the pion can be defined via the same universal formula involving bilocal quark operators [70, 71, 114–116] (in Appendix A we discuss possible more general definitions related to the Lorentz decomposition of the amplitude [17]), namely

$$\begin{aligned} & \int_{-\infty}^{\infty} \frac{d\lambda}{4\pi} e^{i\lambda y p \cdot n} \langle \pi^b(p+q) | \bar{\psi}_\alpha(-\frac{\lambda}{2}n) \not{n} \psi_\beta(\frac{\lambda}{2}n) | \pi^a(p) \rangle \\ & = \delta^{ab} \delta_{\alpha\beta} \mathcal{H}^{I=0}(y, \zeta, t, n^2) + i\epsilon^{abc} \tau_{\alpha\beta}^c \mathcal{H}^{I=1}(y, \zeta, t, n^2), \end{aligned} \quad (1)$$

where a , b , and c are the isospin indices, α and β are the quark flavors (summation over color is implicit), and the subscripts $I = 0, 1$ denote the isospin. As is routinely being done in low-energy chiral quark models, the gauge link operators are omitted, as one does not consider gluons at the quark model scale. Furthermore, the ingoing and outgoing pions are on the mass shell, t is the momentum transfer, and ζ is the skewness parameter:

$$p^2 = m_\pi^2, \quad p \cdot n = 1, \quad q \cdot n = -\zeta, \quad q^2 = -2p \cdot q = t. \quad (2)$$

The momentum fraction carried by the quark is denoted as

$$y = \frac{k \cdot n}{p \cdot n}. \quad (3)$$

For the GPDs, the quarks are separated by a light-like (null) vector λn , i.e., $n^2 = 0$ (then y is traditionally written as the Bjorken x), whereas for qGPDs we have a space-like separation, with $n^2 < 0$, in certain harmony with the Euclidean nature of these objects on the lattice.

For the valence transversity case, tGPD and qtGPD are defined via an analogous formula to Eq. (1), with an additional tensorial structure pulled out:

$$\begin{aligned} & \int \frac{d\lambda}{4\pi} e^{i\lambda y p \cdot n} \langle \pi^b(p+q) | \bar{\psi}_\alpha(-\frac{\lambda}{2}n) n_\mu \sigma^{\mu\nu} \gamma_5 \psi_\beta(\frac{\lambda}{2}n) | \pi^a(p) \rangle \\ & = \epsilon^{npqv} [\delta^{ab} \delta_{\alpha\beta} \mathcal{E}^{I=0}(y, \zeta, t, n^2) \\ & \quad + i\epsilon^{abc} \tau_{\alpha\beta}^c \mathcal{E}^{I=1}(y, \zeta, t, n^2)], \end{aligned} \quad (4)$$

where $\epsilon^{npqv} = \epsilon^{\rho\sigma\lambda\nu} n_\rho p_\sigma q_\lambda$ involves the Levi-Civita tensor with the convention $\epsilon^{0123} = -1$. Note that this definition leads to $\mathcal{E}^{I=0,1}$ of dimension of inverse mass¹, while $\mathcal{H}^{I=0,1}$ are dimensionless. For the GPD or tGPD case, Eqs. (1,4) define the leading twist-2 distributions in the pion.

¹ This can be compensated by multiplying with the mass of the hadron, but we chose not to do it, as it is not usable for the pion in the chiral limit. Also, physical observables involve the whole matrix element, where the issue does not arise.

The definitions (1) and (4) are fully relativistically covariant, and so is our evaluation. However, in Appendix B we provide some possible explicit kinematic assignments to the vectors p , q , and n , defining various reference frames. In particular, for the kinematics used by Ji [1], where the pion moves with momentum P_z and $n = (0, 0, 0, -1/P_z)$, one has

$$n^2 = -\frac{1}{P_z^2}. \quad (5)$$

With the skewness $1 \geq \zeta \geq 0$, and when $n^2 = 0$ (the GPD and tGPD cases), the momentum fraction is bounded $x \in [-1 + \zeta, 1]$ and has three distinct subdomains: $[-1 + \zeta, 0]$, $[0, \zeta]$, and $[\zeta, 1]$, corresponding to three distinct virtual processes: excitement and de-excitement of the antiquark, excitement of a quark-antiquark pair, and excitement and de-excitement of a quark, respectively. On the contrary, for $n^2 < 0$ (the qGPD and qtGPD cases), the momentum fraction y is unbounded, $y \in (-\infty, \infty)$, and the above-mentioned kinematic regions are not sharply separated.

B. Asymmetric and symmetric conventions

Two conventions are used in the literature for the momentum fractions (y, Y) and the skewness (ζ, ξ), which can be determined relative to the incident pion momentum, or to the average momentum of the incident and outgoing pions. These two sets are related by

$$Y = \frac{2y - \zeta}{2 - \zeta}, \quad \xi = \frac{\zeta}{2 - \zeta}. \quad (6)$$

The variables Y and ξ correspond the so-called symmetric convention, because of the symmetry or antisymmetry of the qGPDs about $Y = 0$, whereas y and ζ relate to the asymmetric convention. In this paper we use the symbols H and E to represent qGPDs and tqGPDs in the symmetric convention, while \mathcal{H} and \mathcal{E} are used for the asymmetric convention. Switching between the two conventions amounts to the replacement

$$H^{I=0,1}(Y, \xi, t, n^2) = \mathcal{H}^{I=0,1}(y, \zeta, t, n^2), \quad (7)$$

$$E^{I=0,1}(Y, \xi, t, n^2) = \frac{1}{1 + \xi} \mathcal{E}^{I=0,1}(y, \zeta, t, n^2). \quad (8)$$

We note that according to definition (1) the normalization is $\int dy \mathcal{H}^{I=1}(y, \zeta, t = 0, n^2) = 1 + \zeta/2$, hence $\mathcal{H}^{I=1}$ is not normalized to 1 (the conserved charge of the pion). That feature could be enforced by altering Eq. (1), putting instead of $1/(4\pi)$ the factor $1/[2\pi(2 - \zeta)]$. Then that factor would be canceled in Eq. (7) by the Jacobian of the transformation from y to Y , which is $dy/dY = 2 - \zeta = 1/(1 + \xi)$. The traditional convention, however, uses Eqs. (1,7) as written, with $\int dY H^{I=0,1}(Y, \xi, t = 0, n^2) = 1$. For $E^{I=0,1}$ there is no conservation law enforcing normalization. Nevertheless, with definition (4) and the Jacobian kept in Eq. (8)

the normalization of $E^{I=0,1}(Y, \xi, t = 0, n^2)$ is independent of ξ . Further discussion of related issues is given in subsection III D.

We will occasionally use a short-hand notation, where \mathcal{F} stands for $\mathcal{H}^{I=0,1}$ or $\mathcal{E}^{I=0,1}$, and similarly F stands for $H^{I=0,1}$ or $E^{I=0,1}$. The basic symmetry features of qGPDs in the symmetric notation are

$$\begin{aligned} F^{I=0}(Y, \xi, t, n^2) &= -F^{I=0}(-Y, \xi, t, n^2), \\ F^{I=1}(Y, \xi, t, n^2) &= F^{I=1}(-Y, \xi, t, n^2). \end{aligned} \quad (9)$$

The corresponding quark and antiquark qGPDs and qtGPDs are constructed with the relations

$$\begin{aligned} \mathcal{F}_q(y, \zeta, t, n^2) &= \frac{1}{2} (\mathcal{F}_{I=0}(y, \zeta, t, n^2) + \mathcal{F}_{I=1}(y, \zeta, t, n^2)), \\ \mathcal{F}_{\bar{q}}(y, \zeta, t, n^2) &= \frac{1}{2} (\mathcal{F}_{I=0}(y, \zeta, t, n^2) - \mathcal{F}_{I=1}(y, \zeta, t, n^2)), \end{aligned} \quad (10)$$

and analogously for the symmetric notation.

For GPDs and tGPDs, $x \in [-1 + \zeta, 0] \cup [\zeta, 1]$, or $X \in [-1, -\xi] \cup [\xi, 1]$, is referred to as the DGLAP region, whereas $x \in [0, \zeta]$, or $X \in [-\xi, \xi]$, as the ERBL region, with the names borrowed from the corresponding Dokshitzer-Gribov-Lipatov-Altarelli-Parisi QCD evolution equations for the PDFs and the Efremov-Radyshkin-Brodsky-Lepage evolution for the DAs [117, 118].

C. Polynomiality

An important formal property of qGPDs is the polynomiality feature, whereby the Y -moments of F are even polynomials in the ξ variable, with the coefficients $A_m^{(k)}$ and $B_m^{(k)}$, depending on t and n^2 , interpreted as the generalized quasi form factors:

$$\begin{aligned} \int_{-\infty}^{\infty} dY Y^{2k} H^{I=1}(Y, \xi, t, n^2) &= \sum_{m=0}^k A_m^{(k)}(t, n^2) \xi^{2m}, \\ \int_{-\infty}^{\infty} dY Y^{2k+1} H^{I=0}(Y, \xi, t, n^2) &= \sum_{m=0}^{k+1} B_m^{(k)}(t, n^2) \xi^{2m}, \\ \int_{-\infty}^{\infty} dY Y^{2k} E^{I=1}(Y, \xi, t, n^2) &= \sum_{m=0}^k A_{Tm}^{(k)}(t, n^2) \xi^{2m}, \\ \int_{-\infty}^{\infty} dY Y^{2k+1} E^{I=0}(Y, \xi, t, n^2) &= \sum_{m=0}^{k+1} B_{Tm}^{(k)}(t, n^2) \xi^{2m}. \end{aligned} \quad (11)$$

Polynomiality follows from the basic field theoretic features of the theory, such as the Lorentz covariance, time reversal, and hermiticity, in a full analogy to the GPD case ($n^2 = 0$). The simple derivation proceeds via the double distributions [119], which now are additionally functions of n^2 . This n^2 dependence is carried over to the form factors.

In Appendix E we explicitly check polynomiality for the basic one-loop functions entering the NJL evaluation. Clearly, in the limit of $n^2 \rightarrow 0$ the generalized quasi form factors $A_m^{(k)}(t, n^2)$ and $B_m^{(k)}(t, n^2)$ tend to the generalized form factors related to the GPDs (for a detailed discussion of these quantities and their QCD evolution see [120]).

The zeroth moment of $H^{I=1}$ is independent of n^2 ,

$$\int_{-\infty}^{\infty} dY H^{I=1}(Y, \xi, t, n^2) = A_0^{(0)}(t) = 2F_V(t), \quad (12)$$

where $F_V(t)$ is the pion's charge form factor. Similarly,

$$\int_{-\infty}^{\infty} dY E^{I=1}(Y, \xi, t, n^2) = A_{T0}^{(0)}(t), \quad (13)$$

$$\int_{-\infty}^{\infty} dY E^{I=0}(Y, \xi, t, n^2) = B_{T0}^{(0)}(t), \quad (14)$$

are independent of n^2 . The higher moments do depend explicitly on n^2 .²

The first moment of $H^{I=0}$ involves the gravitational form factors $\theta_{1,2}$ [46]:

$$\int_{-\infty}^{\infty} dY Y H^{I=0}(Y, \xi, t, n^2) = \theta_2(t, n^2) - \xi^2 \theta_1(t, n^2). \quad (15)$$

At the quark model scale, where the quarks are the only degrees of freedom, one has $\theta_2(t = 0, n^2 = 0) = 1$, which reflects the fact that the trace of the energy-momentum tensor in the pion state is m_π^2 [46] (the energy-momentum sum rule). In the chiral limit, a low-energy theorem [121] yields a general relation $\theta_2(t, n^2 = 0) - \theta_1(t, n^2 = 0) = \mathcal{O}(m_\pi^2)$. We note that in the mechanistic interpretation $\theta_1(t)$ is the D -term [122].

D. Generalized Ioffe-time distributions

The generalized ITDs are obtained from qGPDs or qtGPDs via the Fourier transform from the momentum-fraction variables to the Ioffe time ν :

$$\begin{aligned} \mathcal{F}_I(-\nu, \zeta, t, -z^2) &= \int dy e^{i\nu y} \mathcal{F}(y, \zeta, t, z^2/\nu^2), \\ F_I(-\nu, \xi, t, -z^2) &= \int dY e^{i\nu Y} F(Y, \xi, t, z^2/\nu^2), \end{aligned} \quad (16)$$

where the subscript I stands for ‘‘Ioffe’’ and, as already mentioned, \mathcal{F} stands either for $\mathcal{H}^{I=0,1}$ or $\mathcal{E}^{I=0,1}$, while F either for $H^{I=0,1}$ or $E^{I=0,1}$. The Ioffe time is defined as

$$\nu = p \cdot z, \quad (17)$$

² We note, however, that the higher moments in Y may not exist due to the long-range tails in Y of the $F(Y, \xi, t, n^2)$ distributions. As a matter of fact, in the employed NJL model with two Pauli-Villars subtractions we may compute, depending on the type of distribution, the first few Y -moments according to Eq. (36).

which in the employed kinematics is $\nu = -P_z z_3$, hence $\nu^2 = P_z^2 z_3^2 = z^2/n^2$. The variables ν and $z^2 \leq 0$ are the arguments of ITDs. An obvious relation between the asymmetric and symmetric notation follows from Eq. (6), namely

$$F_I(-\nu, \xi, t, -z^2) = e^{-i\nu\xi} \mathcal{F}_I \left[-(1+\xi)\nu, \frac{2\xi}{1+\xi}, t, -z^2 \right], \quad (18)$$

hence for non-zero ξ the real and imaginary parts of the two conventions mix, while ν gets rescaled.

Another simple fact is that the subsequent derivatives of $F_I(-\nu, \xi, t, -z^2)$ with respect to ν at $\nu \rightarrow 0$ (with $z^2 = \nu^2/n^2$) provide the moments of Eqs. (11). We wish to underline here that although higher moments of qGPDs and tqGPD may not and, in general, do not exist, as remarked in footnote² and elaborated in Appendix E, the corresponding ITDs are nevertheless well defined, as a Fourier transform of a regular function that asymptotically goes to zero always exists. The point is, however, that one cannot use it to obtain the higher (non-existing) moments, as one cannot interchange the limit of taking the derivatives and the improper integration. The problem disappears for the GPD limit, as the finite support in x make all moments exist.

With the notation (5) we have (interpreting P_z as fixed)

$$F_I(-\nu, \xi, t, \nu^2/P_z^2) = \int dY e^{i\nu Y} F(Y, \xi, t, -1/P_z^2). \quad (19)$$

Taking $z = (0, 0, 0, z_3)$, whereby $\nu = -z_3 P_z$, one can also write

$$F_I(z_3 P_z, \xi, t, z_3^2) = \int dY e^{-iz_3 P_z Y} F(Y, \xi, t, -1/P_z^2) \quad (20)$$

and treat the ITDs as functions of z_3 at fixed P_z . Due to the rotational invariance, z_3^2 should be viewed as the modulus squared of the space part of z , namely $|z|^2$. In particular, one can choose z in the transverse direction, where it is related to the k_T -unintegrated distributions via Fourier transform.

The generalized *reduced* Ioffe-time distributions [17] are defined as

$$\begin{aligned} \mathfrak{F}(-\nu, \xi, t, -z^2) &= \frac{F_I(-\nu, \xi, t, -z^2)}{F_I(0, \xi, t, -z^2)} \\ &= \frac{\int dY e^{i\nu Y} F(Y, \xi, t, z^2/\nu^2)}{\int dY F(Y, \xi, t, z^2/\nu^2)}, \end{aligned} \quad (21)$$

or

$$\mathfrak{F}(z_3 P_z, \xi, t, z_3^2) = \frac{\int dY e^{-iz_3 P_z Y} F(Y, \xi, t, -1/P_z^2)}{\int dY F(Y, \xi, t, -1/P_z^2)}. \quad (22)$$

These quantities can be efficiently used to probe the transverse-longitudinal factorization [17, 46]. Their Y -moments are independent of P_z up to the rank 1 (see the discussion in subsection III D). Moreover, the reduced distributions are advantageous for the lattice QCD simulations [17].

E. Generalized pseudo-distributions

Radyushkin's pseudo-distributions [15, 16, 123, 124] are in turn defined as Fourier transforms of the ITDs from ν to the momentum fraction x , namely

$$F_P(x, \xi, t, -z^2) = \int \frac{d\nu}{2\pi} e^{-i\nu x} F_I(-\nu, \xi, t, -z^2) \quad (23)$$

(and similarly for the asymmetric convention), where the superscript P stand for ‘‘pseudo’’. An advantage of these distributions is that the momentum fraction has the support $x \in [-1, 1]$ (cf. Appendix G). Moreover, the $x \in [0, 1]$ range corresponding to the quarks is strictly separated from the $x \in [-1, 0]$ region corresponding to the antiquarks. The functional dependence on x and z^2 in the generalized pseudo-distributions can be used to probe the correlation between the longitudinal and transverse dynamics, since in the case of no correlations the x and z^2 dependence factorizes. Clearly, from the definitions it follows that $F_P(x, \xi, t, -z^2 = 0) = F(x, \xi, t, n^2 = 0)$.

F. Relation to k_T -unintegrated GPDs

Another property of pGPDs is their simple relation to the k_T -unintegrated GPDs (or the transverse-momentum distributions (TMDs), up to the intricacies of the Wilson link operators [125]). This feature, derived by Radyushkin [15, 16, 123, 124] and following solely from the Lorentz covariance, naturally generalizes to the pGPD case. The k_T -unintegrated GPDs can be defined as a Fourier transform of the generalized pseudo-distributions as follows:

$$F_T(x, \xi, t, k_1^2 + k_2^2) = \int \frac{dz_1 dz_2}{(2\pi)^2} e^{ik_1 z_1 + ik_2 z_2} F_P(x, \xi, t, z_1^2 + z_2^2), \quad (24)$$

where indices 1, 2 relate to the transverse space. The generalization of the Radyushkin relation, written invariantly, reads

$$F(Y, \xi, t, n^2) = \frac{1}{\sqrt{-n^2}} \int dk_1 \int dx F_T \left[x, \xi, t, k_1^2 - \frac{(x-Y)^2}{n^2} \right]. \quad (25)$$

An explicit check for the one-loop calculation is provided in Appendix F.

The relation of the generalized pseudo or quasi distributions to the k_T -unintegrated generalized distributions opens the possibility of carrying out the QCD evolution with the approach suggested by Kwieciński [110–113], as already done for the qGPDs of both the pion and the nucleon in [46]. This interesting problem is left for a future study.

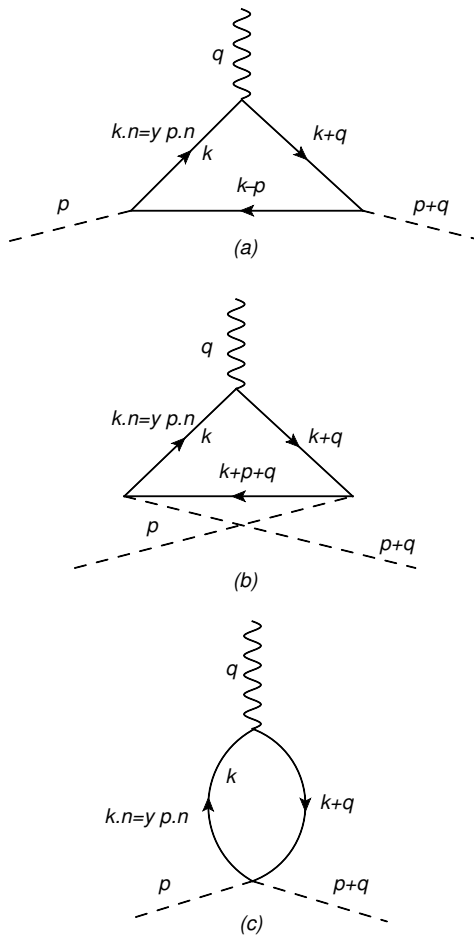


FIG. 1. One-loop diagrams for the evaluation of qGPDs and qtGPDs in the NJL model. Solid lines indicate the quark propagator and dashed lines the external on-shell pions. The wavy line denotes the probing operator \not{n} or $n_\mu \sigma^{\mu\nu} \gamma_5$ for qGPDs or qtGPDs, respectively. The loop momentum integration is over three dimensions only, with the constraint $k \cdot n = y p \cdot n$ eliminating the fourth.

III. VALENCE GPDS AND TGPDS OF THE PION IN THE NJL MODEL

This Section presents novel analytic and semi-analytic results, specific to the NJL model in the large- N_c limit, i.e., obtained at the one-quark-loop level. All the discussion concerns the valence distributions at the quark model scale.

A. Lagrangian

In this subsection we describe the calculation and present the results for the valence qGPDs and qtGPDs of the pion in the NJL model. We apply the non-linear version of the model with the Lagrangian of the form

$$\mathcal{L} = \bar{\psi} (i\not{\partial} - MU^5 - m) \psi, \quad (26)$$

with

$$U^5 = \exp(i\gamma_5 \boldsymbol{\tau} \cdot \boldsymbol{\phi}/f), \quad (27)$$

where M is the constituent quarks mass from the spontaneous chiral symmetry breaking, m is the current quark mass explicitly breaking the chiral symmetry, f is the pion weak decay constant, $\boldsymbol{\tau}$ are the Pauli matrices, and $\boldsymbol{\phi}$ is the pion field. When departing from the strict chiral limit, the canonical pion field becomes $\pi = Z\phi$, such that the canonical pion-quark coupling constant obtained from the residue at the pole of the pion propagator is $g_{\pi q} = ZM/f$ (see [44] for details).

B. Methodology

Our methodology follows the numerous earlier works on the properties of the pion: PDF [60, 61, 126], the distribution amplitude [127], the generalized distribution functions [90], the generalized form factors [120], the quasi distribution amplitude [45], the quasi or pseudo PDFs [46], as well as the double distribution functions [128]. The calculation at the large- N_c level amounts to the evaluation of one-loop diagrams displayed in the Fig. 1. We note that diagram (c), appearing in the non-linear model (26) for nonzero q , makes the result covariant and contributes to the D -term [116].³

The results are interpreted as pertaining to the *quark-model scale*, where the quarks are the only dynamical degrees of freedom. This scale is very low, ~ 320 MeV, as can be assessed from the momentum fraction carried by the valence quarks [90], as well as independently from the value of the quark condensate [129]. There is a demand for the QCD evolution whenever one wishes to compare the model results to the experimental or lattice data at much higher scales. The results at the quark model scale, as those presented in this work, are treated as initial conditions for the QCD evolution, with only valence quarks present. One carries out the evolution to a higher scale, say 2 GeV, whereby sea quarks and gluons are radiatively generated. The program has been carried out for the PDFs [60, 61], GPDs [90], tGPDs [92], and qPDFs [46]. For the present case of qGPDs and tqGPDs, it is left for a future study.

The NJL model is a non-renormalizable effective field-theoretical Lagrangian, hence a high-energy cut-off must be introduced. A way to do it consistently, with the Lorentz and gauge symmetries preserved, is to use a twice-subtracted Pauli-Villars (PV) regularization [44]. In this set up, the basic scalar loop integrals $L(M^2)$ are

³ In the linear σ -like model following from the bosonization of the NJL model, the diagram equivalent to Fig. 1(c) involves a σ -meson propagator in the t -channel. The results at non-zero t are somewhat more complicated from the present ones, but the essentials are the same.

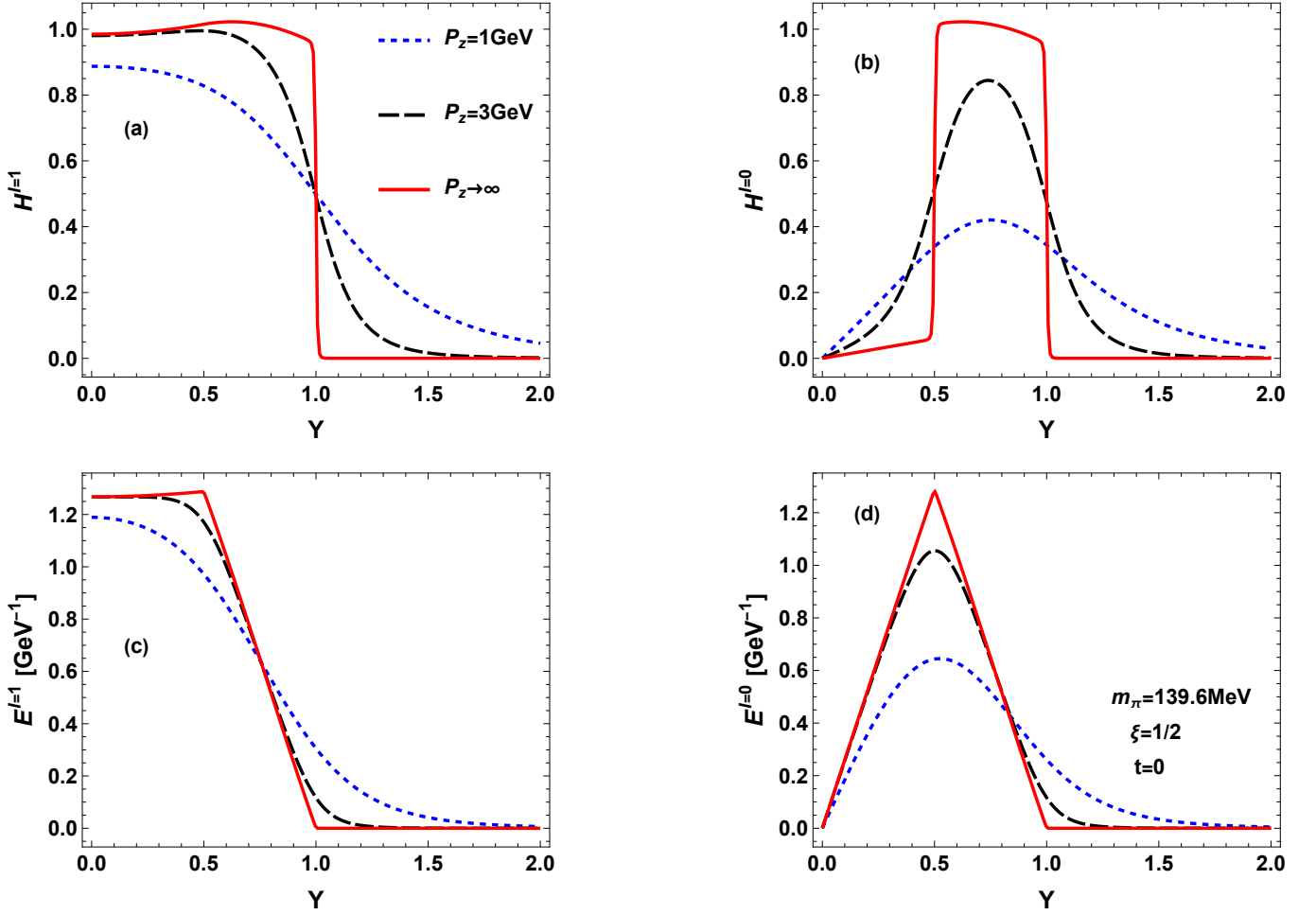


FIG. 2. qGPDs $H^{I=0,1}$ and qtGPDs $E^{I=0,1}$, plotted as functions of Y for several values of P_z (physical pion mass, $\xi = 1/2$, and $t = 0$).

regularized in the following way:

$$L(M^2)_{\text{reg}} = L(M^2) - L(M^2 + \Lambda^2) + \Lambda^2 \frac{dL(M^2 + \Lambda^2)}{d\Lambda^2}. \quad (28)$$

In deriving the one-loop NJL expressions for the qGPDs and tqGPDs we follow exactly the same steps as given in Ref. [90]. Some details are provided in Appendix C. The amplitudes obtained from the subsequent diagrams of Fig. 1 are

$$\begin{aligned} \mathcal{H}^a(y, \zeta, t, n^2) &= \frac{iN_c g_{\pi q}^2}{4\pi^4} \int d^4k \frac{\delta(k \cdot n - y)}{D_k D_{k+q} D_{k-p}} \times \\ &\quad [(k^2 - M^2)(\zeta - y - 1) + k \cdot p(2y - \zeta) - k \cdot q - \frac{1}{2}yt], \\ \mathcal{H}^b(y, \zeta, t, n^2) &= \frac{iN_c g_{\pi q}^2}{4\pi^4} \int d^4k \frac{\delta(k \cdot n - y)}{D_k D_{k+q} D_{k+p+q}} \times \\ &\quad [(k^2 - M^2)(1 - y) - k \cdot p(2y - \zeta) + k \cdot q(1 - 2y - \frac{1}{2}yt)], \\ \mathcal{H}^c(y, \zeta, t, n^2) &= \frac{iN_c g_{\pi q}^2}{4\pi^4} \int d^4k \frac{\delta(k \cdot n - y)}{D_k D_{k+q}} (2y - \zeta), \end{aligned} \quad (29)$$

where, $D_\ell = \ell^2 - M^2 + i0$, and the superscripts correspond to the labels in Fig. 1. For the proper isospin combinations one has

$$\begin{aligned} \mathcal{H}^{I=0} &= \mathcal{H}_a + \mathcal{H}_b + \mathcal{H}_c, \\ \mathcal{H}^{I=1} &= \mathcal{H}_a - \mathcal{H}_b, \end{aligned} \quad (30)$$

and explicitly

$$\begin{aligned} \mathcal{H}^{I=0,1}(y, \zeta, t, n^2) &= \frac{-iN_c g_{\pi q}^2}{8\pi^4} \int d^4k \delta(k \cdot n - y) \quad (31) \\ &\quad \left(\frac{1}{D_k D_{k-p}} + \frac{1 - \zeta}{D_{k+q} D_{k-p}} \mp \frac{1}{D_{k+q} D_{k+q+p}} \mp \frac{1 - \zeta}{D_k D_{k+p+q}} \right. \\ &\quad \left. + \frac{(\zeta - 2y)m_\pi^2 + t(y - 1)}{D_k D_{k+q} D_{k-p}} \mp \frac{(\zeta - 2y)m_\pi^2 + t(y - \zeta + 1)}{D_k D_{k+q} D_{k+p+q}} \right). \end{aligned}$$

Analogously, the amplitudes corresponding to the tqGPDs

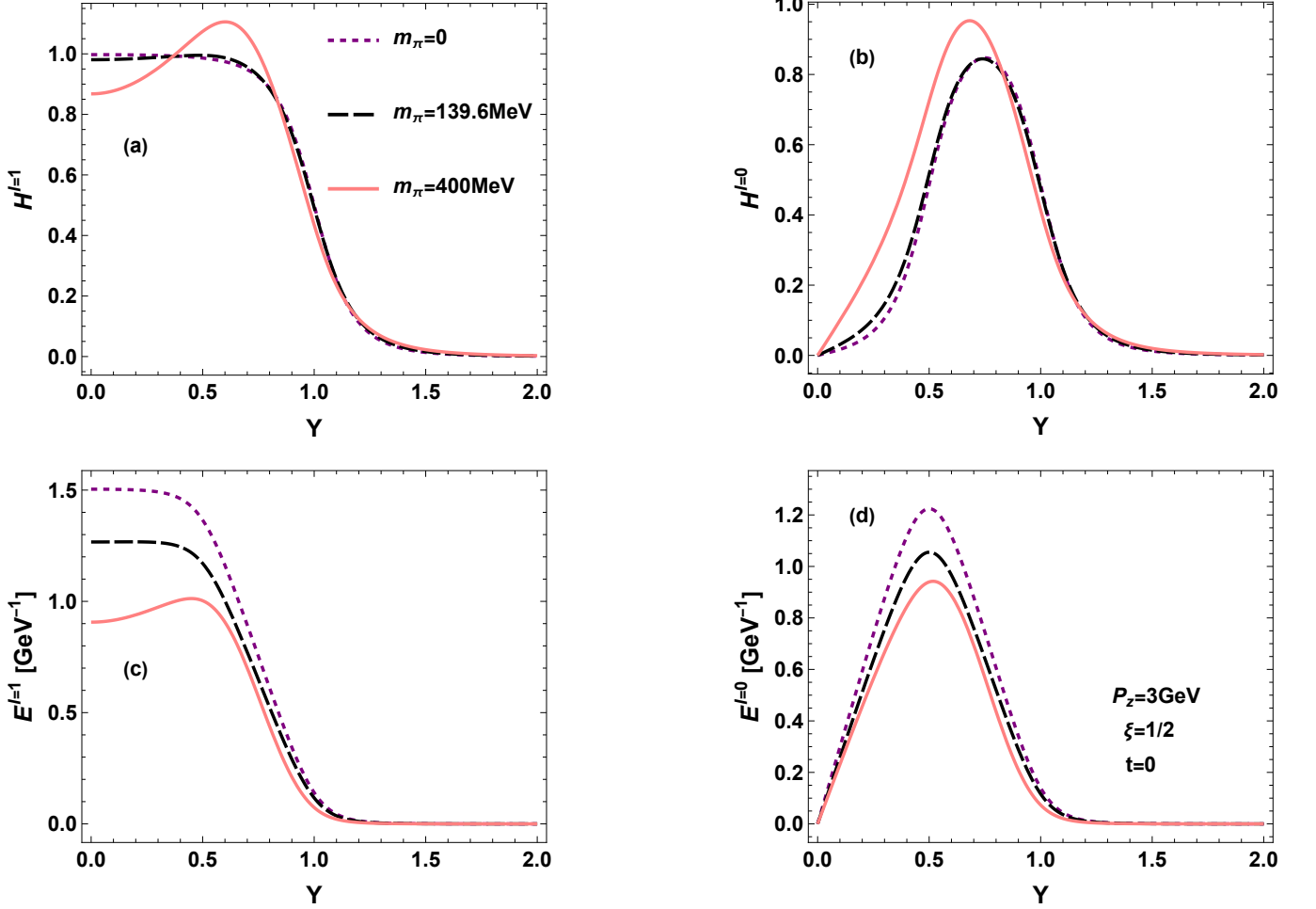


FIG. 3. Same as in Fig. 2, but for a varying pion mass and fixed $P_z = 3$ GeV, $\xi = 1/2$, and $t = 0$.

are

$$\begin{aligned}
 \mathcal{E}^a(y, \zeta, t, n^2) &= \frac{-iN_c M g_{\pi q}^2}{4\pi^4} \int d^4k \frac{\delta(k \cdot n - y)}{D_k D_{k+q} D_{k-p}}, \\
 \mathcal{E}^b(y, \zeta, t, n^2) &= \frac{iN_c M g_{\pi q}^2}{4\pi^4} \int d^4k \frac{\delta(k \cdot n - y)}{D_k D_{k+q} D_{k+p+q}}, \\
 \mathcal{E}^c(y, \zeta, t, n^2) &= 0,
 \end{aligned} \tag{32}$$

Thus, tGPDs get contributions only from the triangle diagrams of Fig. 1. For the isospin combinations one has, in analogy to Eq. (30),

$$\begin{aligned}
 \mathcal{E}^{I=0,1}(y, \zeta, t, n^2) &= \frac{-iN_c M g_{\pi q}^2}{4\pi^4} \int d^4k \delta(k \cdot n - y) \\
 &\left(\frac{1}{D_k D_{k+q} D_{k-p}} \mp \frac{1}{D_k D_{k+q} D_{k+p+q}} \right).
 \end{aligned} \tag{33}$$

From the form of Eqs. (31) and (33) it is clear that we need to evaluate two types of integrals: the scalar two-point function (bubble) I and the three-point function (triangle) J (see the Appendix C for the definitions and evaluation). Substituting these in Eqs. (31) and (33) yields our final expressions used for computations:

$$\begin{aligned}
\mathcal{H}^{I=0,1}(y, \zeta, t, n^2) &= \frac{1}{2} \left[I(y, 1, m_\pi^2) + (1 - \zeta) I(y - \zeta, 1 - \zeta, m_\pi^2, n^2) \mp I(y - \zeta, -1, m_\pi^2) \mp (1 - \zeta) I(y, \zeta - 1, m_\pi^2, n^2) \right. \\
&\quad \left. - [(\zeta - 2y)m_\pi^2 + t(y - 1)] J\left(y, \zeta, 1, t, m_\pi^2, -\frac{t}{2}, n^2\right) \mp [(\zeta - 2y)m_\pi^2 + t(y + 1 - \zeta)] J\left(\zeta - y, \zeta, 1, t, m_\pi^2, -\frac{t}{2}, n^2\right) \right] \\
\mathcal{E}^{I=0,1}(y, \zeta, t, n^2) &= \frac{M}{2} \left[J\left(y, \zeta, 1, t, m_\pi^2, -\frac{t}{2}, n^2\right) \mp J\left(\zeta - y, \zeta, 1, t, m_\pi^2, -\frac{t}{2}, n^2\right) \right].
\end{aligned} \tag{34}$$

TABLE I. The values of the parameters used in the present work and the resulting values of the pion mass, pion weak decay constant, and the pion-quark coupling constant.

	M [MeV]	m [MeV]	Λ [MeV]	m_π [MeV]	f_π [MeV]	$g_{\pi q}$
chiral	300	0	731	0	86	3.49
physical	300	7.5	830	139.6	93	3.14
lattice	300	41.5	1115	400	110	2.29

The above formulas are generic for the evaluation based on the diagrams of Fig. 1, with the model details (such as the choice of regularization in the NJL model or the selection of parameters) contained in the basic one-loop functions I and J . We note the Lorentz invariance and proper crossing symmetry properties.

In the GPD or tGPD case ($n^2 = 0$), the above distributions for $I = 0$ and $I = 1$ differ by functions whose support vanishes in the positive DGLAP region (cf. Appendix C). Therefore, in the NJL model at the quark-model scale the $I = 0, 1$ GPDs or tGPDs are equal in the positive DGLAP region, and equal and opposite in the negative DGLAP region. In the symmetric notation

$$F^{I=0}(X, \xi, t, n^2 = 0) = \text{sgn}(X) F^{I=1}(X, \xi, t, n^2 = 0), \quad \text{for } |X| > \xi. \tag{35}$$

For $n^2 < 0$ the formula does not hold, as the supports of the one-loop functions are not separated. Also, the QCD evolution, working differently in the singlet and non-singlet cases, breaks it, so Eq. (35) holds specifically at the quark-model scale.

In the spontaneously broken phase, the model has three parameters: the constituent quark mass M , the current quark mass m , and the cut-off parameter Λ used in the PV regularization of the scalar loop diagrams. Following the standard procedure, two of these (m and Λ) are fixed by demanding particular values of m_π and f_π , whereas M is set to 300 MeV. The values of the parameters used in the present work are listed in Table I. ‘‘Chiral’’ corresponds to the chiral limit, ‘‘physical’’ to the charged pion mass, and ‘‘lattice’’ to a large pion mass, of the order of the values used in some less expensive lattice QCD simulations.

C. Quasi GPDs and tGPDs

In this subsection we present qGPDs and qtGPD obtained in the NJL model. Since the prime objective of the paper is an investigation of the dependence of the results on P_z , with the lattice feasibility in mind, we begin by showing in Fig. 2 $H^{I=0,1}$ and $E^{I=0,1}$ as functions of Y . We use here the physical pion mass, fixed sample values of $\xi = 1/2$ and $t = 0$, and several representative values of P_z . We remark that $P_z \sim 3$ GeV is about the upper limit accessible in the present-day lattice studies. Clearly, the limit $P_z \rightarrow \infty$ corresponds to GPDs or tGPDs. In the model, the GPDs and tGPD have sharp edges at $x = \xi$ and at the end-points $x = \pm 1$ [90, 92] (see Appendix D). Finite value of P_z washes out these discontinuities, thus covering up the finer details of the distributions. We note that at $P_z = 1$ GeV we are far from the $P_z \rightarrow \infty$ limit, whereas $P_z = 3$ GeV gets significantly closer. The discrepancy is larger for the case of $H^{I=0,1}$ rather than for $E^{I=0,1}$.

For finite P_z , at asymptotic Y we find for the NJL model with two PV subtractions the behavior

$$\begin{aligned}
H^{I=1} &\sim |Y|^{-5}, & H^{I=0} &\sim Y^{-6}, \\
E^{I=1} &\sim |Y|^{-7}, & E^{I=0} &\sim Y^{-8}.
\end{aligned} \tag{36}$$

According to the discussion in subsection II C, this limits the ranks of the nonzero Y -moments up to 2, 3, 4 and 5 for $H^{I=1}$, $H^{I=0}$, $E^{I=1}$, and $E^{I=0}$, respectively.

In Fig. 3 we show an analogous study of the dependence on the pion mass, with fixed $P_z \sim 3$ GeV, and with $\xi = 1/2$ and $t = 0$. In some lattice QCD simulations one uses a large pion mass, $\sim 300 - 400$ MeV, which requires less statistics. Thus we present as well the case of a large pion mass, $m_\pi = 400$ MeV. The effect of large m_π is particularly significant for $E^{I=1}$, but noticeable also for all the other cases.

The effect of changing ξ is not shown separately to not proliferate the number of figures. It just moves the discontinuities of the GPDs or tGPDs at the value $X = \xi$, with the quasi distribution following them, similarly as in Fig. 2. Naturally, it affects the slopes. The dependence on the momentum transfer t is discussed in detail on the case of the generalized quasi form factors in Sec. III D.

TABLE II. Values of the rms radii of various form factors for the three considered values of m_π .

m_π [MeV]	0	139.6	400
$\langle r^2 \rangle_V^{1/2}$ [fm]	0.54	0.52	0.50
$\langle r^2 \rangle_{A^{(0)}}^{1/2}$ [fm]	0.53	0.53	0.58
$\langle r^2 \rangle_{B_{T0}^{(0)}}^{1/2}$ [fm]	0.41	0.41	0.49
$\langle r^2 \rangle_{\theta_1}^{1/2}$ [fm] ($P_z = 1$)	0.57	0.56	0.62
$\langle r^2 \rangle_{\theta_1}^{1/2}$ [fm] ($P_z \rightarrow \infty$)	0.38	0.36	0.32
$\langle r^2 \rangle_{\theta_2}^{1/2}$ [fm] ($P_z = 1$)	0.30	0.28	0.32
$\langle r^2 \rangle_{\theta_2}^{1/2}$ [fm] ($P_z \rightarrow \infty$)	0.38	0.37	0.39

D. Generalized quasi form factors

According to Eqs. (11), qGPDs and qtGPDs may be thought of as infinite collections of the generalized quasi form factors. In this subsection we analyze the lowest generalized quasi form factors, as they should possibly be accessible to lattice determinations. The properties of the generalized form factors related to GPDs, in particular their QCD evolution, were discussed in detail in [130], whereas the chiral quark model predictions were reported in [120].

We start with the form factors which are independent of n^2 , namely $A_0^{(0)}(t) = 2F_V(t)$, $A_{T0}^{(0)}(t)$, and $B_{T0}^{(0)}(t)$. They are shown in Fig. 4 for three values of m_π . The mean squared radii are defined generically as

$$\langle r^2 \rangle = \frac{6}{F(0)} \left. \frac{dF(t)}{dt} \right|_{t=0}, \quad (37)$$

and the corresponding root mean squared (rms) radii are collected for several form factors in Table II.

For the vector form factor of Fig. 4(a) we note a mild decrement of the rms radius with m_π . The lower number compared to the experiment, $(0.659(4) \text{ fm})^2$ [131], is attributed to the missing chiral loops in our leading $1/N_c$ treatment.

The lowest order form factors of qtGPDs are shown in Fig. 4(b,c). In our model, the values at the origin are \mathcal{N} for $A_{T0}^{(0)}(t)$ and $\mathcal{N}/3$ for $B_{T0}^{(0)}(t)$, where \mathcal{N} is given in Eq. (D3). The corresponding rms radii for the $I = 1$ form factor, $A_{T0}^{(0)}$, are similar to the vector case.

The two quasi gravitational form factors are presented in Fig. 5. Unlike the above-discussed cases, these form factors do depend on P_z . What is independent of P_z , however, is the value of θ_2 at the origin, $\theta_2(0, n^2) = 1$. This model result is more general than the energy momentum sum-rule mentioned in subsection II C, holding for the $n^2 = 0$ case. Also, in our model in the chiral limit $\theta_1(t, n^2) - \theta_2(t, n^2) = \mathcal{O}(m_\pi^2)$ for any n^2 , extending the similar low energy theorem for light-like vectors, $n^2 = 0$.

The values of the rms radii of the quasi gravitational form factors given in Table II exhibit a strong dependence on P_z , which is complementary to the behavior in Fig. 5.

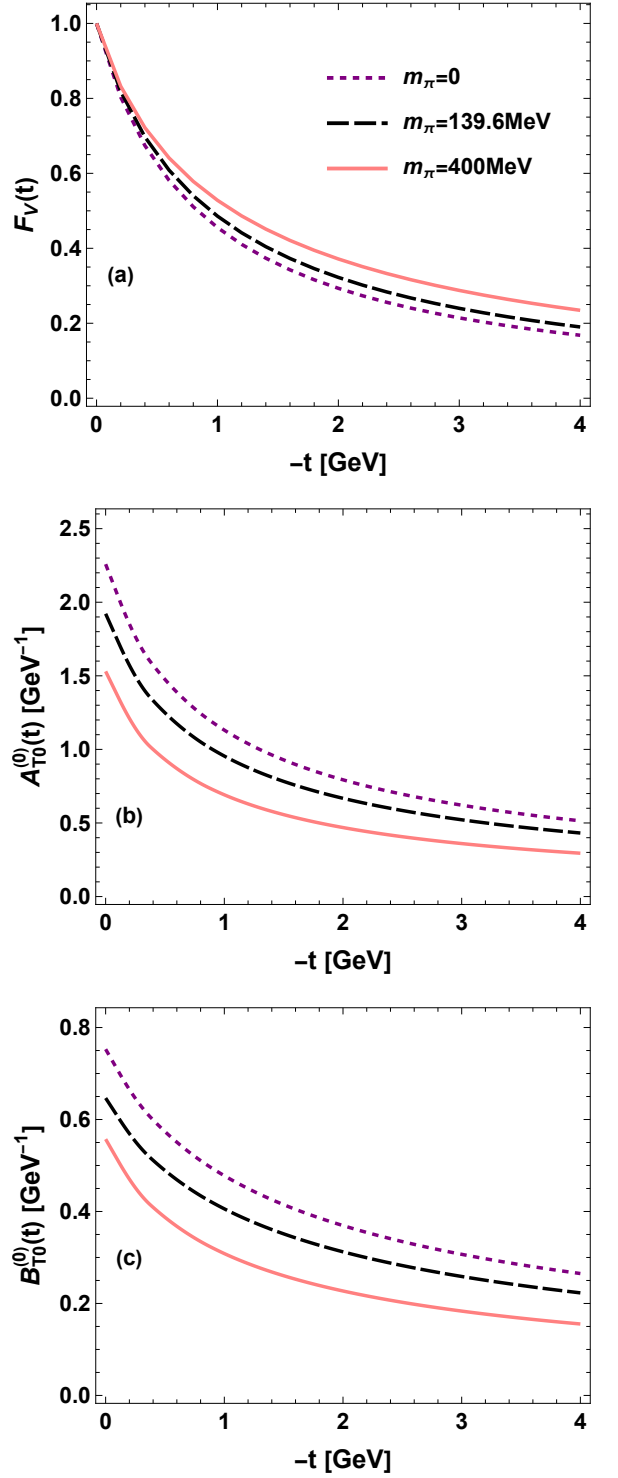


FIG. 4. Form factors independent of n^2 , plotted at space-like momentum transfer t for several values of the pion mass.

We note that the model relation showing a more compact distribution of matter than charge in the pion [120],

$$2\langle r^2 \rangle_{\theta_{1,2}} = \langle r^2 \rangle_V, \quad (38)$$

holds for $n^2 = 0$ and in the chiral limit.

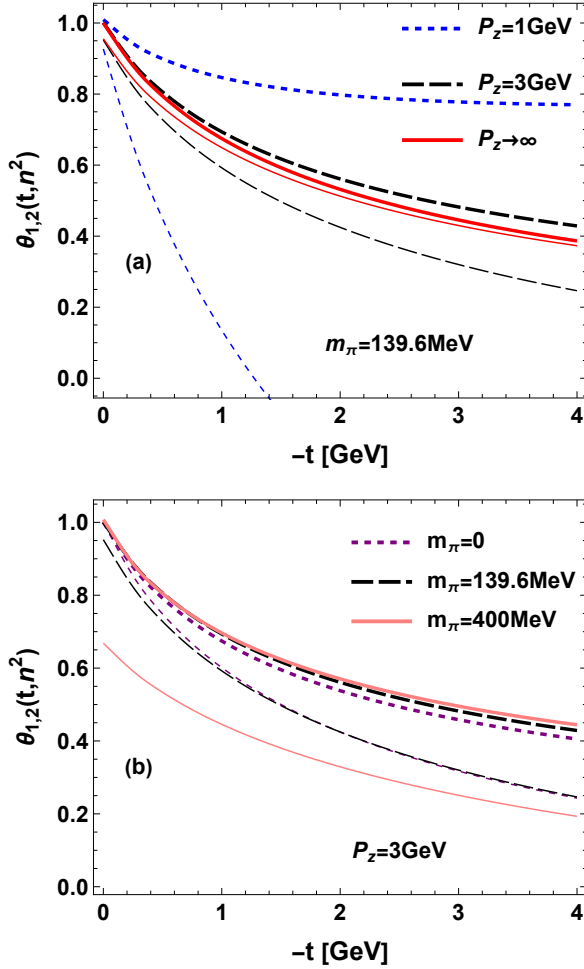


FIG. 5. Quasi gravitational form factors θ_1 (thin lines) and θ_2 (thick lines) for (a) various values of P_z at the physical pion mass, and (b) for various pion masses at $P_z = 3$ GeV.

There is yet another relevant feature pertaining to the form factors discussed up to now. The vector form factor, corresponding to a conserved current, does not evolve with the QCD scale. The QCD evolution of the generalized form factors (for $n^2 = 0$) is multiplicative for the gravitational form factors (albeit the quark pieces mix with the gluon distributions), hence the valence form factors change only by an overall factor, whereas their shape in t is preserved. Analogously, for the rank-0 form factors of $E^{I=0,1}$ the renormalization is multiplicative, hence their shape in t is preserved. This feature is generally not preserved for the higher rank generalized form factors, whose LO QCD evolution mixes them [130]. Therefore we encounter a situation where the higher rank generalized quasi form factors not only strongly depend on n , but also are largely affected by the QCD evolution. For their assessment at higher scales, carrying out the evolution is necessary.

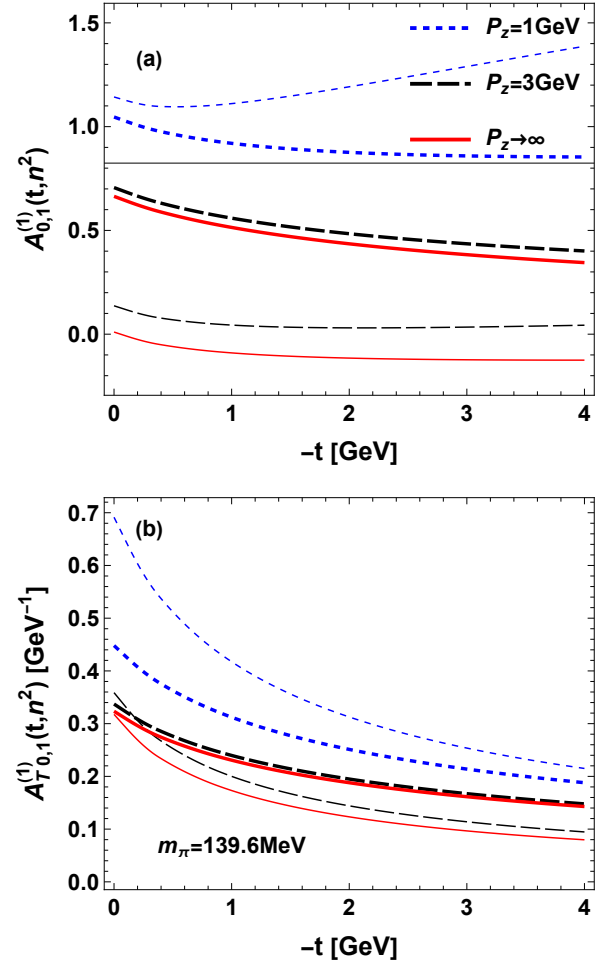


FIG. 6. Sample higher-order generalized quasi form factors.

E. Generalized Ioffe-time distributions

In this subsection we show our model results for the reduced generalized ITDs defined in Eq. (21) for each of the functions $H^{I=1,0}$ and $E^{I=1,0}$. We discuss them in detail, as they have become basic objects of the lattice QCD studies. From symmetry properties in ν , the $I = 1$ parts are purely real, and the $I = 0$ parts purely imaginary, so we do not have to carry the isospin labels in the notation. The (reduced) ITD of Eq. (21) are in general functions of, independently, $-\nu$ and $-z^2$, but following [17] we take the sections defined by $-z^2 = \nu^2/P_z^2$. First, we investigate the dependence of the reduced ITDs on P_z .

In the NJL model, the one-loop expressions for the generalized ITDs follow from the simple formulas of Appendix G. It is clear that in the chiral limit and for $t = 0$ the dependence on $z_3 = \sqrt{-z^2}$ and ν is separated, as z_3 appears only in the argument of the Bessel functions $K_{0,1}(z_3 M)$. Therefore the dependence on $z_3 = \nu/P_z$ cancels out from the ratio in Eq. (21) and the results for \mathfrak{H} and \mathfrak{E} do not depend on P_z . On the contrary, the ITDs (not reduced) would display a strong non-separability of ν and z_3 , obscuring the picture [17].

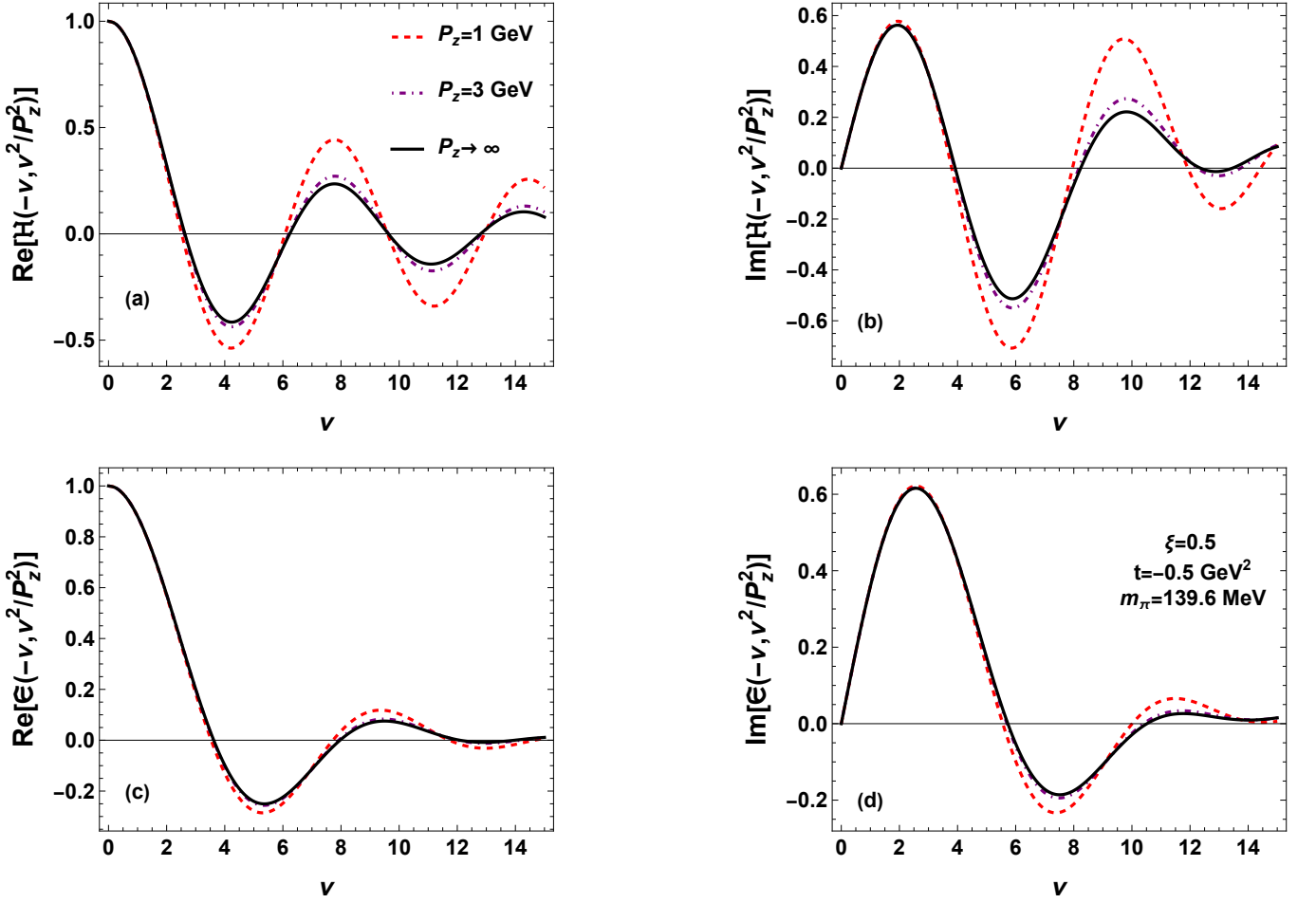


FIG. 7. Real and imaginary parts of the reduced generalized ITDs of the pion, plotted as functions of ν at $z_3 = \nu/P_z$ for various values P_z . Physical pion mass, $t = -0.5\text{GeV}^2$, and $\xi = 1/2$.

In the chiral limit and for $t = 0$, the following formulas are derived in Appendix D:

$$\begin{aligned} \mathfrak{H} &= \frac{\sin \nu}{\nu} + i \frac{\cos \nu \xi - \cos \nu}{\nu}, \\ \mathfrak{E} &= 2 \frac{\cos \nu \xi - \cos \nu}{\nu^2(1 - \xi^2)} + 2i \frac{\xi \sin \nu - \sin \nu \xi}{\nu^2 \xi(1 - \xi^2)}, \end{aligned} \quad (39)$$

where the real and imaginary parts correspond to the $I = 1$ and $I = 0$ pieces, respectively. Of course, the independence of P_z here is manifest.

Nonzero values of m_π or t cause a due breaking of the ν - z_3 separability, as can be clearly seen from Fig. 7 made for the physical pion mass, a moderate $t = -0.5 \text{ GeV}^2$, and $\xi = 1/2$. The breaking is more prominent at larger values of ν , as expected from the fact that the second argument is ν^2/P_z^2 . While for the displayed range of ν the difference between $P_z = 1 \text{ GeV}$ and $P_z \rightarrow \infty$ is substantial, the results for $P_z = 3 \text{ GeV}$ essentially coincide with the GPD limit of $P_z \rightarrow \infty$.

Next, we pass to studying the dependence of the generalized ITDs on ξ . The expansion of formulas (39) at

$\nu = 0$ yields (at $m_\pi = 0$ and $t = 0$)

$$\begin{aligned} \mathfrak{H} &= \sum_{k=0}^{\infty} \frac{\nu^{2k}}{(2k+1)!} + i \sum_{k=0}^{\infty} (-1)^k \frac{\nu^{2k+1}(1 - \xi^{2k+2})}{(2k+2)!}, \\ \mathfrak{E} &= \sum_{k=0}^{\infty} (-1)^k \frac{2\nu^{2k} p_k(\xi^2)}{(2k+2)!} + i \sum_{k=0}^{\infty} (-1)^k \frac{2\nu^{2k+1} p_k(\xi^2)}{(2k+3)!}, \end{aligned} \quad (40)$$

where $p_k(\xi^2) = 1 + \xi^2 + \dots + \xi^{2k}$, and explicitly

$$\begin{aligned} \mathfrak{H} &= 1 - \frac{1}{6}\nu^2 + i \left[\frac{1}{2}(1 - \xi^2)\nu - \frac{1}{24}(1 - \xi^4)\nu^3 \right] + \dots, \\ \mathfrak{E} &= 1 - \frac{1}{12}(1 + \xi^2)\nu^2 + i \left[\frac{1}{3}\nu - \frac{1}{60}(1 + \xi^2)\nu^3 \right] + \dots \end{aligned} \quad (41)$$

We note the manifestation of polynomiality in the above expressions in their dependence on ξ . In the case of general m_π and t , in the limit of $P_z \rightarrow \infty$ the coefficients of the expansion of the generalized ITDs relate to the X -moments of the corresponding GPDs, hence provide the information on the generalized form factors.

For the case shown in Fig. 8, prepared with the physical pion mass, $t = -0.5$, and $P_z = 3 \text{ GeV}$, the results

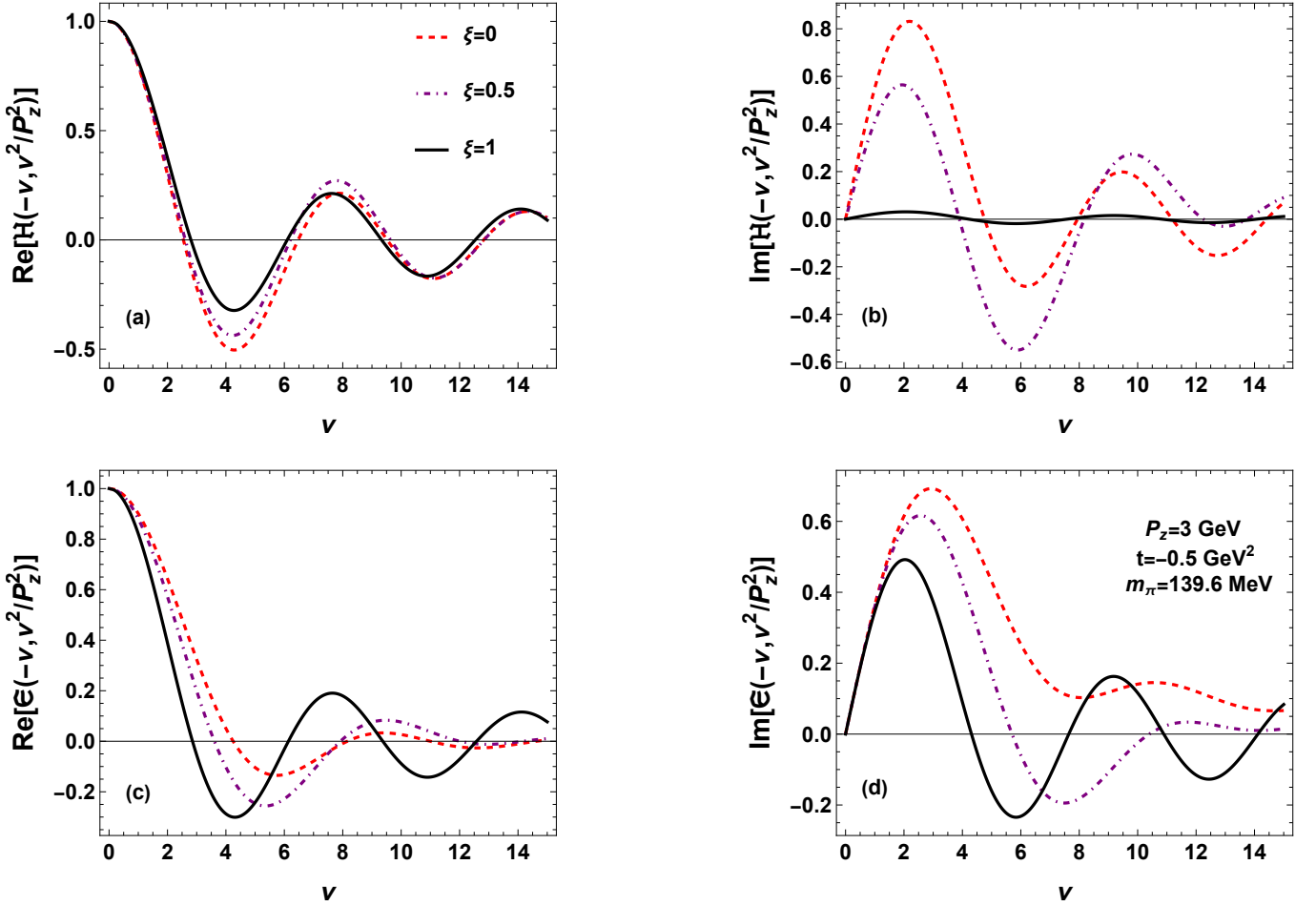


FIG. 8. Same as in Fig. 7 but for different values of the skewness parameter ξ . Physical pion mass, $t = -0.5 \text{ GeV}^2$, and $P_z = 3 \text{ GeV}$.

are not too far away from the case of Eqs. (39), hence we note the characteristic approximate features, such as the weak dependence of $\text{Re}(\mathfrak{H})$ on ξ , the nearly zero $\text{Im}(\mathfrak{H})$, the proportionality of the slope of $\text{Im}(\mathfrak{H})$ to $(1 - \xi^2)$, the increase of the curvature of $\text{Re}(\mathfrak{E})$ as $(1 + \xi^2)$, and the independence of the slope of $\text{Im}(\mathfrak{E})$ of ξ . In general, we note that, as expected from the framework, the dependence on ξ is certainly a relevant feature. Methodologically, this can be used as an alternative way to obtain the generalized form factors.

In Figs. 9 and 10 we examine the dependence of the generalized ITDs on the value of m_π and t for the fixed value of $P_z = 3 \text{ GeV}$. The features directly reflect the appearance of m_π and t in Eqs. (34). We find that the dependence on m_π is very moderate, even with the large value of $m_\pi = 400 \text{ MeV}$. The differences are a bit larger for \mathfrak{H} than for \mathfrak{E} . On the other hand, the dependence on t is somewhat more substantial, partly because we have taken as moderate the value of $-t = 0.5 \text{ GeV}^2$, which, however, is significantly larger than the used values of m_π^2 .

F. Generalized pseudo-distributions

First, we notice that equalities analogous to Eq. (35) hold for the generalized pseudo-distributions in the DGLAP region for any value of z_3 :

$$F_P^{I=0}(X, \xi, t, -z_3^2) = \text{sgn}(X) F_P^{I=1}(X, \xi, t, -z_3^2), \quad \text{for } |X| > \xi. \quad (42)$$

The reason is a proper separation of the supports of the loop functions provided in Appendix G

In Fig. 11 we show the generalized pseudo-distributions of Eq. (23) obtained in our model for the physical m_π , $t = 0$, and skewness $\xi = 1/2$, plotted as functions of x for three sample values of z_3 . We can vividly see that in the DGLAP region the generalized pseudo-distributions coincide, according to Eq. (42). The case of $z_3 \rightarrow 0$ corresponds, naturally, to the GPDs or tGPDs. We note that with increasing z_3 , the distributions decrease, which is naturally attributed to the pseudo form factor in z_3 , defined as $F_P(x, \xi, t, z_3^2)/F_P(x, \xi, t, 0)$.

From the form of Eqs. (G2) and (G4) it is clear that in our model, for $m_\pi = 0$ and $t = 0$, the dependence on

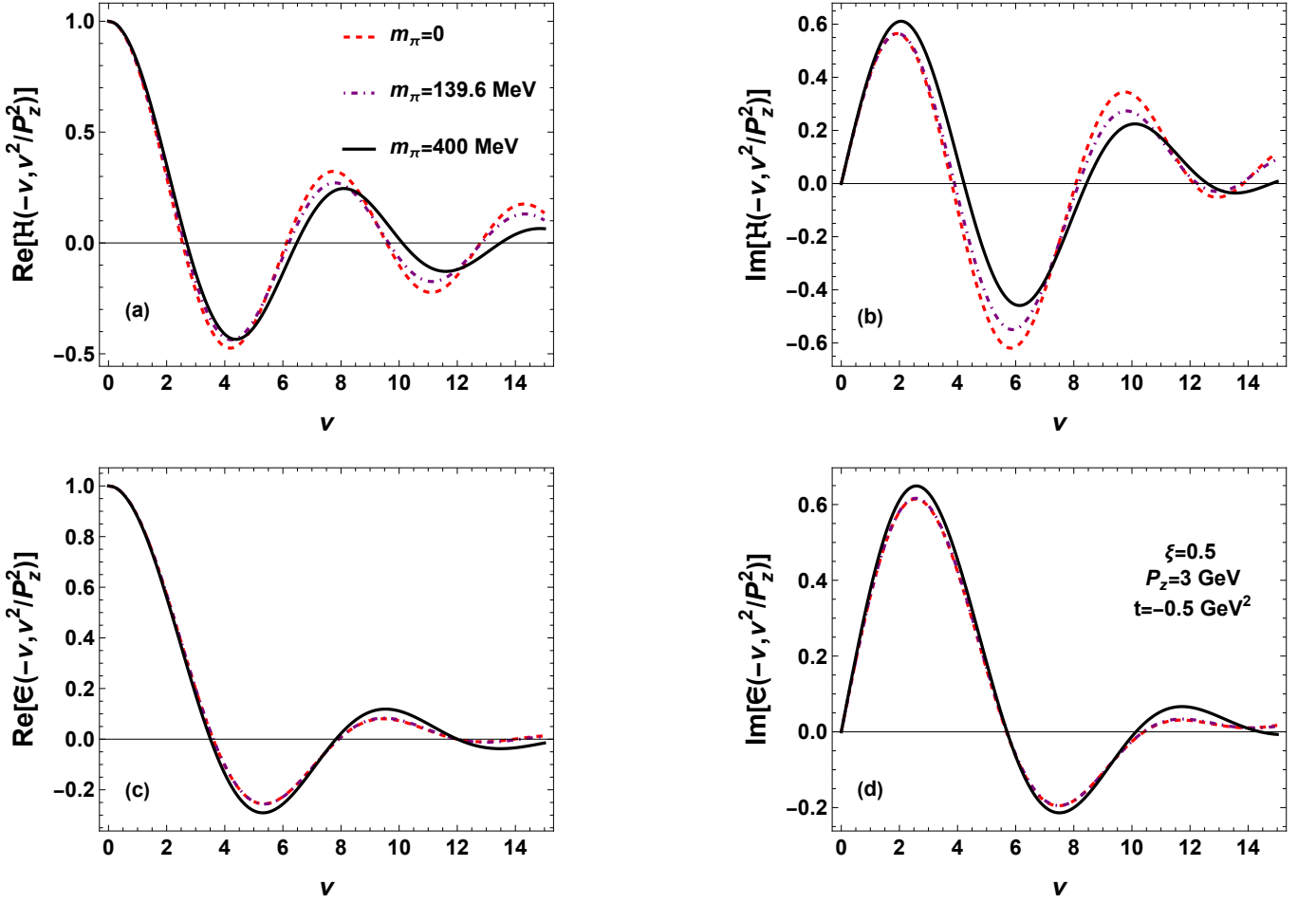


FIG. 9. Same as in Fig. 7 but for different values of the pion mass at $\xi = 0.5$, $t = -0.5 \text{ GeV}^2$, and $P_z = 3 \text{ GeV}$.

x and $z^2 = -z_3^2$ factorizes. Then the shape of the generalized pseudo-distributions is given by Eqs. (D1,D2), supplied with a universal (x -independent) pseudo form factor in z_3^2 . For the case of a general kinematics the factorization no longer holds exactly, but it still nearly holds for the physical value of m_π and small values of $-t$. At larger values of $-t$ it becomes visibly broken. This is manifest in Fig. 12, where the form factor is plotted for the physical pion mass, $\xi = 0.5$, and $t = -0.5 \text{ GeV}^2$, for several values of x , both in the DGLAP and ERBL region. In the DGLAP region (here we take $x = 2/3$), the form factors for the $I = 0$ and $I = 1$ cases are identical, as follows directly from Eq. (42). In the ERBL region we notice the breaking, which essentially is due to the taken value of $-t$ (whereas $m_\pi^2 \simeq 0.02 \text{ GeV}^2$, a very small number).

We also note from Fig. 12 that the breaking is stronger for the H pseudo form factors than for the E case. This feature reflects the structure of Eq. (34), where t multiplies the J functions in the definition of H , but not for E , thus contributing to stronger breaking of the factorization.

As the Fourier transform from z to k_T converts the

generalized pseudo-distributions into the generalized k_T -unintegrated distributions (cf. Eq. (24)), the plots of Fig. 12 provide also complementary information on the k_T -unintegrated GPDs and tGPDs. In particular, the curvature of the pseudo form factors at the origin yields the average transverse momentum squared, $\langle k_T^2 \rangle(x, \xi, t)$, in the k_T -unintegrated GPDs and tGPDs.

Finally, we wish to discuss the range of $|\nu|$, denoted as ν_{\max} , needed to carry out the inverse Fourier transform in definition (23). This is of practical importance, as in numerical evaluation such as in the lattice QCD simulations, unlike our analytic case, we always have an upper bound for $|\nu|$. From Fig. 11 we can see that the rate of variation of the pseudo-distributions is about $\Delta = \min(\xi, 1 - \xi)$ for $0 < \xi < 1$, and $\Delta = 1$ for $\xi = 0$ or $\xi = 1$ (the pseudo-PDF or the pseudo-DA limit). For the Fourier transform to be able to reproduce it, we need $\nu_{\max} \gg 2\pi/\Delta$. Thus, for a fixed ν_{\max} more accurate results would follow for $\xi = 1/2$ than for ξ close (but not equal) to 0 or 1. For $\xi = 1/2$ we need $\nu_{\max} \gg 4\pi$, so at least of the order of 30, depending on the demanded accuracy. Such large values are presently prohibitive for the lattice QCD simulations.

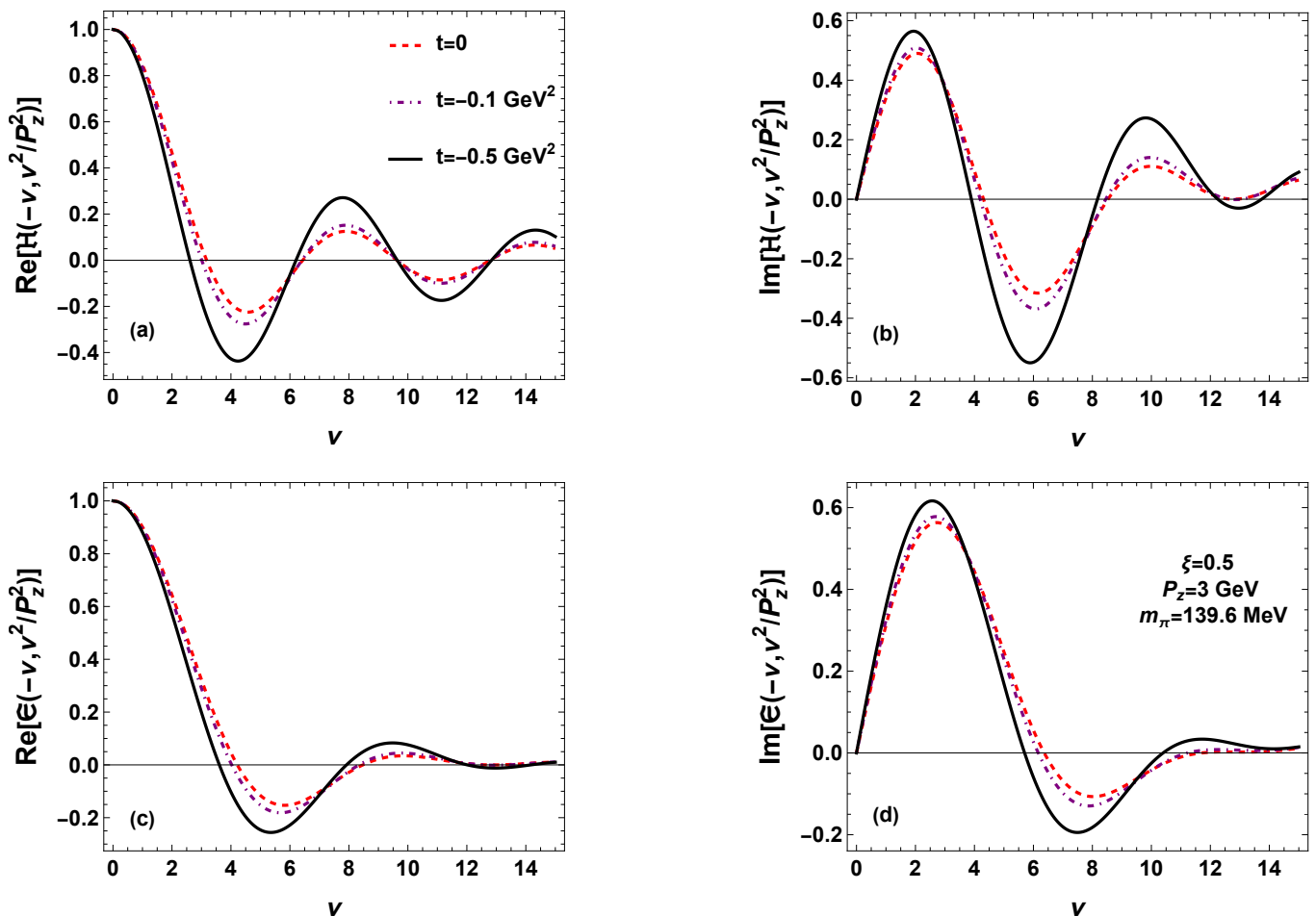


FIG. 10. Same as in Fig. 7 but for different momentum transfer t at the physical pion mass, $\xi = 0.5$, and $P_z = 3$ GeV.

We remark that a similar problem occurs in the “good lattice cross section” method [28, 29], where also large values of the Ioffe-time are necessary [132] to provide a reliable information on the higher x -moments.

IV. CONCLUSIONS

We have carried out an extensive analysis of the quasi GPDs and tGPDs, related generalized Ioffe-time distributions, and generalized pseudo distributions of the pion in the framework of the NJL model. Even in this very simple model, treated at the one-quark-loop (large- N_c) level, the results are nontrivial and reveal the rich structure of the examined objects.

Of particular interest is the dependence of the results on the momentum of the pion, P_z . Referring to the ITDs, which are the quantities directly accessible in the lattice QCD simulations, we find that $P_z = 3$ GeV is sufficiently close (within a few percent) to the desired limit of $P_z \rightarrow \infty$ for low-enough values of the Ioffe time $\nu < 15$, while the case $P_z = 1$ GeV is still significantly away (cf. Fig. 7). This is especially so for the case of

non-zero skewness, where more variation is present in the distributions, in particular the isoscalar GPDs. We stress that the conclusion that $P_z \simeq 3$ GeV is large enough for ITDs does not carry over to the qGPDs themselves (cf. Fig. 2), where much larger values would be necessary, say, $P_z > 10$ GeV, depending on how closely one wishes to approximate the $P_z \rightarrow \infty$ limit near the endpoints and near $Y = \pm\xi$. The issue is related to the general difficulties in accurately Fourier transforming the ITDs into qGPDs with a limited accessible range in the Ioffe time, as discussed at the end of Sec. III F.

Our estimates may be useful for implementations of the skewed quasi distributions on the lattice, which are yet to come. We have also studied the dependence on the pion mass, including a large value of 400 MeV, which is in the range of values used some lattice QCD studies.

We have computed quasi generalized form factors, related to moments of the qGPDs and qtGPDs, and investigated their dependence on P_z . Only the lowest rank form factors are independent of P_z , and the higher ones do, in particular, the gravitational form factors, whose shape changes strongly between $P_z = 1$ GeV and 3 GeV. They are also sensitive to m_π .

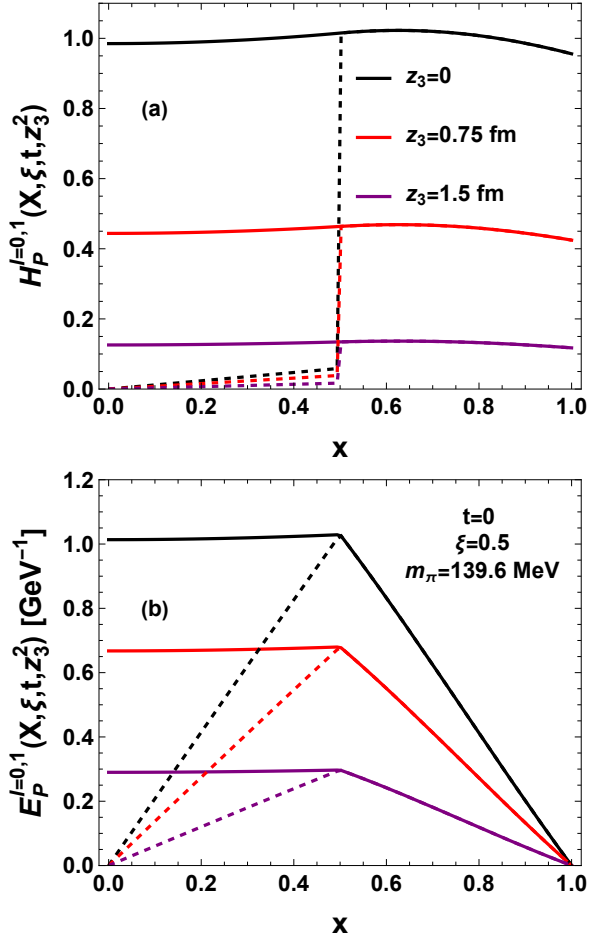


FIG. 11. Generalized pseudo-distributions for the physical pion mass, $t = 0$, and $\xi = 0.5$, plotted as functions of the momentum fraction x for three sample values of z_3 .

The generalized (reduced) Ioffe-time distributions, basic objects for the lattice investigations, encode the information on the quasi-distributions as their Fourier transforms. We have discussed in detail the dependence on the skewness parameter ξ , exhibiting the simple characteristics such as the slope or curvature of certain GPDs or qGPDs.

We have also estimated how large values of the Ioffe time ν_{\max} are needed to effectively invert the Fourier transform to get the pseudo-distributions defined in the x -space. The value of ν_{\max} , should be larger if skewness is present, as it causes larger variation in the qGPDs and qtGPDs. Roughly, values $\nu_{\max} > 30$ are necessary.

With the obtained pseudo distributions, we have investigated the breaking of the longitudinal-transverse separability. The effects of m_π are rather small here, but larger values of the momentum transfer t cause significant breaking. The issue is related to properties of the k_T -unintegrated distributions (or TMDs).

We stress that our analysis is based on analytic or semi-analytic expressions, which allows for a simple insight and illustration of the intricate formal features of the

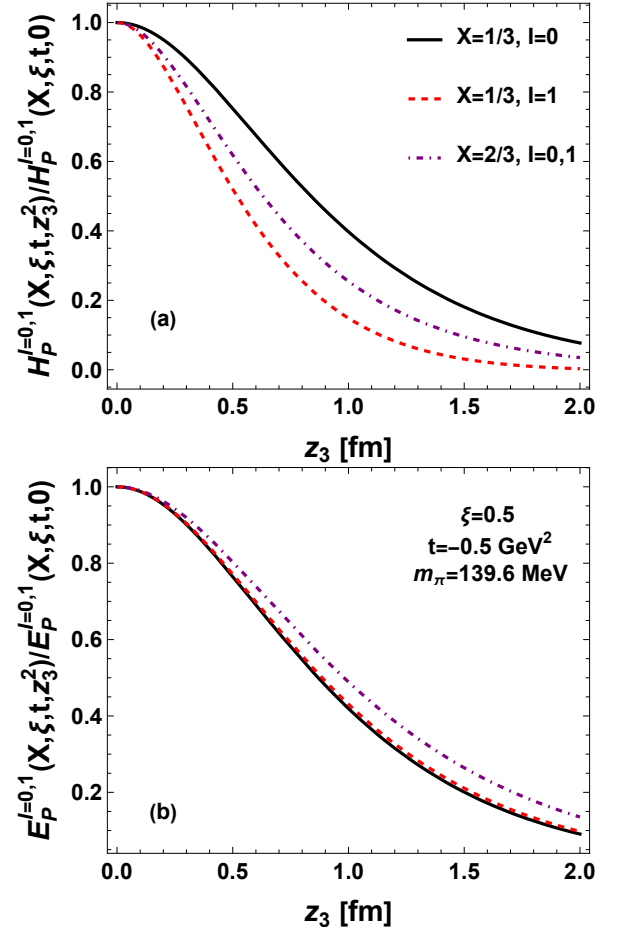


FIG. 12. Pseudo form factors $F_P(x, \xi, t, z_3^2)/F_P(x, \xi, t, 0)$ for the physical pion mass, $t = 0$, and $\xi = 0.5$, plotted as functions of z_3^3 for two sample values of x : one in the DGLAP and one in the ERBL region.

field. At the same time, our results pertain to the quark-model scale, which is much lower from the experimental or lattice scales. In the context of the QCD evolution, we have thus investigated the initial conditions and their sensitivity to P_z , m_π , t , or ξ . That sensitivity will be carried over to higher scales, with the exact effects to be estimated in a future study. With the existing link to the k_T -unintegrated distributions, the QCD evolution of the latter ones can be used to evolve the qGPDs and qtGPDs.

ACKNOWLEDGMENTS

VS acknowledges the support by the Polish National Science Centre (NCN), grant 2019/33/B/ST2/00613. WB acknowledges the support by the Polish National Science Centre, grant 2018/31/B/ST2/01022. ERA acknowledges support from project PID2020-114767GB-I00 funded by MCIN/AEI/10.13039/501100011033 as well as Junta de Andalucía (grant FQM-225).

Appendix A: General Lorentz structure

By Lorentz covariance, the matrix element (we skip the isospin indices for the simplicity of notation)

$$M^\mu = \langle \pi(p+q) | \bar{\psi}(-\frac{\lambda}{2}n) \gamma^\mu \psi(\frac{\lambda}{2}n) | \pi(p) \rangle \quad (\text{A1})$$

can be decomposed as

$$M^\mu = A p^\mu + B q^\mu + C n^\mu, \quad (\text{A2})$$

thus leading to three independent amplitudes, A , B , and C . Explicitly,

$$\begin{aligned} A &= \frac{4(\zeta^2 M_p - n^2 t) - 2M_q(n^2 t - 2\zeta) - 2(\zeta - 2)t M_n}{4m_\pi^2(\zeta^2 - n^2 t) + t(-4\zeta + n^2 t + 4)}, \\ B &= \frac{(4\zeta - 2n^2 t)M_p - 4(m_\pi^2 n^2 - 1)M_q + 2(t - 2\zeta m_\pi^2)M_n}{4m_\pi^2(\zeta^2 - n^2 t) + t(-4\zeta + n^2 t + 4)}, \\ C &= \frac{2(2 - \zeta)t M_p + 2(t - 2\zeta m_\pi^2)M_q + t(t - 4m_\pi^2)M_n}{4m_\pi^2(\zeta^2 - n^2 t) + t(-4\zeta + n^2 t + 4)}, \end{aligned} \quad (\text{A3})$$

where $M_a = M^\mu a_\mu$. Our choice of Eqs. (1,4) corresponds, along the lines of the original proposal by Ji [1], to the combination

$$n_\mu M^\mu = A - \zeta B + n^2 C. \quad (\text{A4})$$

However, as suggested in [17], in view of the lattice QCD implementations it may be advantageous to project out the C term, which would lead to

$$\begin{aligned} A - \zeta B &= \\ \frac{2n^2[(\zeta - 2)t M_p - (t - 2\zeta m_\pi^2)M_q] + 4M_n(\zeta^2 m_\pi^2 - \zeta t + t)}{4m_\pi^2(\zeta^2 - n^2 t) + t(-4\zeta + n^2 t + 4)}. \end{aligned} \quad (\text{A5})$$

Also, the C term of the amplitude is subleading in the twist expansion [17].

Although a consideration of the general or of the projected case (A5) is certainly possible, we do not pursue it here due to algebraic complications, and hold on to the definition (A4).

Appendix B: Kinematics

Whereas our calculations are fully covariant, it is worthwhile to consider specific assignments for the momenta, having in mind possible lattice implementations where a particular reference frame must be specified. Without a loss of generality, we may pick up a frame where the three Lorenz vectors have the t, x, y, z coordinates taken as

$$\begin{aligned} n &= (n_0, 0, 0, n_3), \\ p &= (p_0, 0, 0, p_3), \\ q &= (q_0, q_T, 0, q_3). \end{aligned} \quad (\text{B1})$$

For the n vector, we use the condition (5), where P_z is a *parameter* (not necessarily equal to p_3) controlling how far n is from the null vector case $n^2 = 0$, which corresponds to the limit of $P_z \rightarrow \infty$ (the GPD case). With the choice (B1) we have

$$\epsilon^{npqv} = \delta_{\nu 2}(p_0 n_3 - p_3 n_0) q_T. \quad (\text{B2})$$

Treating p_0 and p_3 as known variables, with $p_0^2 = m_\pi^2 + p_3^2$, and using the total of five conditions from Eq. (2) and (5), we solve the system for n_0, n_3, q_0, q_T , and q_3 , with the result

$$\begin{aligned} n_0 &= \frac{p_0}{m_\pi^2} - \frac{p_3 \sqrt{m_\pi^2 + P_z^2}}{m_\pi^2 P_z}, \\ n_3 &= \frac{p_3}{m_\pi^2} - \frac{p_0 \sqrt{m_\pi^2 + P_z^2}}{m_\pi^2 P_z}, \\ q_0 &= -\frac{p_0 t}{2m_\pi^2} + \frac{p_3 P_z (t - 2\zeta m_\pi^2)}{2m_\pi^2 \sqrt{m_\pi^2 + P_z^2}}, \\ q_3 &= -\frac{p_3 t}{2m_\pi^2} + \frac{p_0 P_z (t - 2\zeta m_\pi^2)}{2m_\pi^2 \sqrt{m_\pi^2 + P_z^2}}, \\ q_T^2 &= \frac{t[\frac{1}{4}t - (1 - \zeta)P_z^2] - m_\pi^2(\zeta^2 P_z^2 + t)}{m_\pi^2 + P_z^2}. \end{aligned} \quad (\text{B3})$$

For the specific choice $P_z = p_3$ [1] Eqs. (B3) reduce to

$$\begin{aligned} n_0 &= 0, \quad n_3 = -\frac{1}{P_z}, \\ q_0 &= -\frac{2\zeta P_z^2 + t}{2p_0}, \quad q_3 = -\zeta P_z, \\ q_T^2 &= \frac{(2\zeta P_z^2 + t)^2}{4p_0^2} - \zeta^2 P_z^2 - t, \end{aligned} \quad (\text{B4})$$

where n is aligned with the z direction. Another potentially useful case is for the initial pion at rest, when

$$\begin{aligned} n_0 &= \frac{1}{m_\pi}, \quad n_3 = -\frac{\sqrt{m_\pi^2 + P_z^2}}{m_\pi P_z}, \\ q_0 &= -\frac{t}{2m_\pi}, \quad q_3 = \frac{P_z(t - 2\zeta m_\pi^2)}{2m_\pi \sqrt{m_\pi^2 + P_z^2}}, \\ q_T^2 &= \frac{t(\frac{1}{4}t - (1 - \zeta)P_z^2) - m_\pi^2(\zeta^2 P_z^2 + t)}{m_\pi^2 + P_z^2}. \end{aligned} \quad (\text{B5})$$

The case of GPDs corresponds to the null vector n , which can be achieved from Eqs. (B3) by taking the limit $P_z \rightarrow \infty$, with the result

$$\begin{aligned} n_0 &= \frac{1}{p_0 + p_3}, \quad n_3 = -\frac{1}{p_0 + p_3}, \\ q_0 &= -\frac{t}{2(p_0 + p_3)} - \zeta p_3, \quad q_3 = \frac{t}{2(p_0 + p_3)} - \zeta p_0, \\ q_T^2 &= (\zeta - 1)t - \zeta^2 m_\pi^2. \end{aligned} \quad (\text{B6})$$

For a physical process all momenta must have real coordinates, in particular q_T must be real. This leads to

constraints, which for the qGPD case at various values of P_z take the form

$$\frac{t}{2} \leq m_\pi^2 + (1 - \zeta)P_z^2 - \sqrt{(m_\pi^2 + P_z^2)(m_\pi^2 + (1 - \zeta)^2 P_z^2)},$$

or

$$(B7)$$

$$\frac{t}{2} \geq m_\pi^2 + (1 - \zeta)P_z^2 + \sqrt{(m_\pi^2 + P_z^2)(m_\pi^2 + (1 - \zeta)^2 P_z^2)}.$$

For the special case of GPD ($P_z \rightarrow \infty$) conditions (B7) reduce to

$$t \leq -\frac{m_\pi^2 \zeta^2}{1 - \zeta}. \quad (B8)$$

This shows that the maximum value of t is (for $\zeta > 0$) strictly less than 0. The reason is that the momentum transfer along n (for $\zeta > 0$) brings in a negative contribution to t .

Appendix C: Evaluation of the loop integrals

In this Appendix we explain for completeness the evaluation of the basic loop integrals. The procedure, us-

ing standard methods, follows closely Ref. [90]. We encounter two types of scalar loop integrals, the two-point function I and the three-point function J , defined below. They are evaluated in the Euclidean space using the Schwinger parameterization of the scalar propagators,

$$S_k = \frac{1}{D_k} = \int_0^\infty e^{-a(k^2 + M^2)}. \quad (C1)$$

Note that in the Euclidean notation used in the Appendices, $p^2 = (p + q)^2 = -m_\pi^2$, $q^2 = -t$, and $n^2 \geq 0$.

1. Two-point function

With the representation (C1) we have

$$\begin{aligned} I(y, \kappa, l^2, n^2) &= 4N_c g_{\pi q}^2 \int \frac{d^4 k}{(2\pi)^4} \frac{\delta(k \cdot n - y)}{D_k D_{k-l}} \\ &= 4N_c g_{\pi q}^2 \int \frac{d^4 k}{(2\pi)^4} \int \frac{d\lambda}{2\pi} e^{i\lambda(k \cdot n - y)} \int_0^\infty d\alpha \int_0^\infty d\beta e^{-\alpha(k^2 + M^2) - \beta((k-l)^2 + M^2)} \\ &= 4N_c g_{\pi q}^2 \int \frac{d^4 k}{(2\pi)^4} \int \frac{d\lambda}{2\pi} \int_0^\infty d\alpha \int_0^\infty d\beta \exp \left[-(\alpha + \beta)(k'^2 + M^2) - \frac{\lambda^2 n^2}{4(\alpha + \beta)} + i \frac{\lambda \beta \kappa}{\alpha + \beta} - \frac{\alpha \beta l^2}{\alpha + \beta} - i\lambda y \right]. \end{aligned} \quad (C2)$$

where the shifted momentum is $k' = k - i \frac{\lambda n}{2(\alpha + \beta)} - \frac{\beta l}{\alpha + \beta}$.

First, we notice that in the case of $n^2 = 0$, the λ integration yields $\delta(y - \frac{\kappa \beta}{\alpha + \beta})$, hence the proper support $\theta[x(\kappa - x)]$ for the momentum fraction $x = y$ follows [90]. However, when (Euclidean) $n^2 > 0$, the λ integral is over a Gaussian with a spread proportional to $\frac{1}{n^2}$. Thus, after the λ integration, we obtain a Gaussian function in y whose width is proportional to n^2 . Clearly, in the limit of $n^2 \rightarrow 0$ we retrieve the result given in Ref. [90].

Next, we use the following change of variables:

$$\begin{aligned} k_T^2 &= k_1'^2 + k_2'^2, \quad K^2 = k_0'^2 + k_3'^2, \\ s &= \alpha + \beta, \quad \psi = \frac{\beta}{s}, \end{aligned} \quad (C3)$$

with $dk_1 dk_2 = \pi dk_T^2$, $dk_0 dk_3 = \pi dK^2$, and $d\alpha d\beta = s ds d\psi$. The integration over K^2 and s yields

$$\begin{aligned} I(y, \kappa, l^2, n^2) &= \frac{N_c g_{\pi q}^2}{8\pi^2 \sqrt{n^2}} \times \\ &\int_0^\infty dk_T^2 \int_0^1 d\psi \frac{1}{[k_T^2 + M^2 + \psi(1 - \psi)l^2 + \frac{1}{n^2}(y - \psi\kappa)^2]^{3/2}}, \end{aligned} \quad (C4)$$

while the further integration over ψ gives the result

$$\begin{aligned} I(y, \kappa, l^2, n^2) &= \frac{N_c g_{\pi q}^2}{4\pi^2 f^2} \int_0^\infty dk_T^2 \times \\ &\frac{\frac{2\kappa y - l^2 n^2}{\sqrt{y^2 + n^2(k_T^2 + w^2)}} + \frac{2\kappa(\kappa - y) - l^2 n^2}{\sqrt{(\kappa - y)^2 + n^2(k_T^2 + w^2)}}}{4[\kappa^2(k_T^2 + w^2) + l^2 y(\kappa - y)] - l^2 n^2 [l^2 + 4(k_T^2 + w^2)]} \end{aligned} \quad (C5)$$

Note the desired symmetry $y \leftrightarrow \kappa - y$.

In the limit of $n^2 = 0$ and $y = x$ we promptly recover the result of Ref. [90]:

$$\begin{aligned} I(y, \kappa, l^2, n^2 = 0) &= \frac{N_c g_{\pi q}^2 \theta[x(\kappa - x)]}{4\pi^2 |\kappa|} \times \\ &\int_0^\infty dk_T^2 \frac{1}{k_T^2 + M^2 + \frac{x}{\kappa} (1 - \frac{x}{\kappa}) l^2}. \end{aligned} \quad (C6)$$

Since the remaining integration over k_T in Eq. (C6) is logarithmically divergent, it can only be carried out after a suitable regularization.

However, curiously, the k_T integration can be carried out in Eq. (C5) where a nonzero n^2 acts as a regulator,

and asymptotically the integrand in Eq. (C5) behaves as $1/k_T^3$. The result of the integration is (we show it explicitly for the case of $l^2 = -m_\pi^2$ encountered in our analysis)

$$I(y, \kappa, -m_\pi^2, n^2) = \frac{N_c g_{\pi q}^2}{4\pi^2} \times \quad (C7)$$

$$\frac{\log \left[\frac{2\sqrt{(\kappa^2 + m_\pi^2 n^2)(n^2 w^2 + (y - \kappa)^2)} - 2\kappa(y - \kappa) + m_\pi^2 n^2}{2\sqrt{(\kappa^2 + m_\pi^2 n^2)(n^2 w^2 + y^2)} - 2\kappa y - m_\pi^2 n^2} \right]}{\sqrt{\kappa^2 + m_\pi^2 n^2}}.$$

This expression can be shown to be symmetric with respect to the replacement $y \leftrightarrow \kappa - y$. It exhibits the expected quark-antiquark production cut for $m_\pi > 2M$. The asymptotic behavior at large $|y|$ is $1/|y|$.

Since for $n^2 > 0$ the k_T integration can be carried out, we can rewrite Eq. (C4) as

$$I(y, \kappa, l^2, n^2) = \frac{N_c g_{\pi q}^2}{4\pi^2 \sqrt{n^2}} \times \quad (C8)$$

$$\int_0^1 d\psi \frac{1}{[M^2 + \psi(1 - \psi)l^2 + \frac{1}{n^2}(y - \psi\kappa)^2]^{1/2}}.$$

Coming back to Eq. (C6), it can be promptly derived

$$J = \frac{3N_c g_{\pi q}^2}{16\pi^2 \sqrt{n^2}} \int_0^1 d\psi \int_0^1 d\tau \int_0^\infty dk_T^2 \frac{\theta(1 - \psi - \tau)}{[k_T^2 + M^2 + \psi(1 - \psi)l^2 + \tau(1 - \tau)l'^2 - 2\psi\tau l \cdot l' + \frac{1}{n^2}(y - \kappa\psi - \kappa'\tau)^2]^{5/2}}$$

$$= \frac{N_c g_{\pi q}^2}{8\pi^2 \sqrt{n^2}} \int_0^1 d\psi \int_0^1 d\tau \frac{\theta(1 - \psi - \tau)}{[M^2 + \psi(1 - \psi)l^2 + \tau(1 - \tau)l'^2 - 2\psi\tau l \cdot l' + \frac{1}{n^2}(y - \kappa\psi - \kappa'\tau)^2]^{3/2}}. \quad (C13)$$

The integral over k_T^2 is finite, hence above it could have been carried out. The integrations over ψ and τ are analytic, but the final results are very lengthy and not instructive, so we do not quote them.

Using Eq. (C9) we find that in the limit of $n^2 \rightarrow 0$

$$J(x, \kappa, \kappa', l^2, l'^2, l \cdot l', 0) = \frac{N_c g_{\pi q}^2}{4\pi^2} \int_0^1 d\psi \int_0^1 d\tau \times \quad (C14)$$

$$\frac{\theta(1 - \psi - \tau) \delta(x - \kappa\psi - \kappa'\tau)}{M^2 + \psi(1 - \psi)l^2 + \tau(1 - \tau)l'^2 - 2\psi\tau l \cdot l'},$$

which agrees with the result of Ref. [90].

Appendix D: GPDs for $m_\pi = 0$ and $t = 0$

The GPD case ($n^2 = 0$) for $m_\pi = 0$ and $t = 0$ yields very simple expressions. For the GPDs we have [90]

$$H^{I=1}(X, \xi) = \theta(1 - X^2), \quad (D1)$$

$$H^{I=0}(X, \xi) = \text{sgn}(X) \theta(1 - X^2) \theta(X^2 - \xi^2),$$

from Eq. (C4) by noticing that it contains the distribution

$$\lim_{n^2 \rightarrow 0} \frac{1}{\sqrt{n^2} (A^2 + \frac{B^2}{n^2})^{3/2}} = \frac{2}{A^2} \delta(B). \quad (C9)$$

2. Three-point function

The scalar triangle integral is defined as

$$J(y, \kappa, \kappa', l^2, l'^2, l \cdot l', n^2) = \quad (C10)$$

$$4N_c g_{\pi q}^2 \int \frac{d^4 k}{(2\pi)^4} \frac{\delta(k \cdot n - y)}{D_k D_{k-l} D_{k-l'}}.$$

Following the procedure from Appendix C 1 for

$$J = 4N_c g_{\pi q}^2 \int \frac{d^4 k}{(2\pi)^4} \int \frac{d\lambda}{2\pi} \int_0^\infty d\alpha \int_0^\infty d\beta \int_0^\infty d\gamma \times \quad (C11)$$

$$e^{i\lambda[k \cdot n - y] - \alpha[k^2 + M^2] - \beta[(k-l)^2 + M^2] - \gamma[(k-l')^2 + M^2]}$$

with

$$s = \alpha + \beta + \gamma, \quad \psi = \beta/s, \quad \tau = \gamma/s, \quad (C12)$$

$$d\alpha d\beta d\gamma = s^2 ds d\psi d\tau,$$

we find

whereas for the tGPDs [92]

$$E^{I=1}(X, \xi) = \mathcal{N} \theta(1 - X^2) \quad (D2)$$

$$\times \left[\theta(|X| - \xi) \frac{|X| - 1}{\xi - 1} + \theta(\xi^2 - X^2) \right],$$

$$E^{I=0}(X, \xi) = \mathcal{N} \theta(1 - X^2)$$

$$\times \left[\text{sgn}(X) \theta(|X| - \xi) \frac{(|X| - 1)}{\xi - 1} + \theta(\xi^2 - X^2) \frac{X}{\xi} \right].$$

The normalization constant is

$$\mathcal{N} = \frac{N_c g_{\pi q}^2 M}{4\pi^2} \frac{1}{M^2} \Big|_{\text{reg.}}, \quad (D3)$$

where in the adopted PV regularization (28)

$$\frac{1}{M^2} \Big|_{\text{reg.}} = \frac{\Lambda^4}{M^2(\Lambda^2 + M^2)^2}. \quad (D4)$$

The corresponding reduced ITDs of Eq. (21) are given in Eq. (39).

Appendix E: Polynomiality

The moments or I and J functions with respect to y are defined as

$$\langle y^m I \rangle = \int_{-\infty}^{\infty} dy y^m I(y, \kappa, l^2, n^2), \quad (\text{E1})$$

$$\langle y^m J \rangle = \int_{-\infty}^{\infty} dy y^m J(y, \kappa, \kappa', l^2, l'^2, l \cdot l', n^2),$$

with $m = 0, 1, 2, \dots$. Taking Eq. (C4) and changing the integration variable to $y' = (y - \kappa\psi)/\sqrt{n^2}$ we can write

$$\langle y^m I \rangle = \frac{N_c g_{\pi q}^2}{8\pi^2} \times \int_{-\infty}^{\infty} dy' \int_0^{\infty} dk_T^2 \int_0^1 d\psi \frac{(\sqrt{n^2} y' + \kappa\psi)^m}{[k_T^2 + M^2 + \psi(1-\psi)l^2 + y'^2]^{3/2}}. \quad (\text{E2})$$

If the integral over y' exists, it is a polynomial of degree m in κ with coefficients given by functions of l^2 and n^2 .

Similarly, with Eq. (C13) and the change of variables $y' = (y - \kappa\psi - \kappa'\tau)/\sqrt{n^2}$, we find that $\langle y^m J \rangle$ is a polynomial in variables κ and κ' of degree m with coefficients given by functions of l^2 , l'^2 , $l \cdot l'$, and n^2 .

After same work, polynomiality of the basic loop integrals translates into polynomiality of the y -moments of qGPDs and qtGPDs for the on-shell pion, which (if exist) are polynomials in ξ with coefficients given by the generalized quasi form factors, which are functions of t and, in general, n^2 .

Appendix F: Radyushkin's relations for the scalar one-loop functions

The relations derived by Radyushkin [15, 16, 123, 124], following entirely from the Lorentz covariance, link nontrivially the quasi-distributions $\tilde{q}(y, n^2)$ to the k_T -unintegrated distributions $q(x, k_T^2)$, namely

$$\tilde{q}(y, n^2) = \frac{1}{\sqrt{n^2}} \int dk_1 \int dx q[x, k_1^2 - \frac{(x-y)^2}{n^2}]. \quad (\text{F1})$$

Here we verify explicitly that these relations hold separately for the basic n -point functions, and hence generalize for the considered quasi-(t)GPDs.

Taking Eq. (C2) and integrating it over dK^2 we can write

$$I(y, \kappa, l^2, n^2) = \frac{N_c g_{\pi q}^2}{4\pi^2} \int_0^{\infty} du \int \frac{d\lambda}{2\pi} \int_0^{\infty} ds \int_0^1 d\psi \times \exp \left[-s(u + M^2) - \frac{\lambda^2 n^2}{4s} + i\lambda\psi\kappa - s\psi(1-\psi)l^2 - i\lambda y \right], \quad (\text{F2})$$

where $u = k_T^2$. On the other hand, the k_T -unintegrated

expression with $\mathbf{k}_T = (k_1, 0)$ and $n^2 = 0$ reads

$$I(x, \kappa, l^2, k_1^2) = \frac{N_c g_{\pi q}^2}{4\pi^3} \int_0^{\infty} dU \int \frac{d\lambda}{2\pi} \int_0^{\infty} s ds \int_0^1 d\psi \times \exp \left[-s(U + k_1^2 + M^2) + i\lambda\psi\kappa - s\psi(1-\psi)l^2 - i\lambda x \right], \quad (\text{F3})$$

where $U = K^2$. Using the identity

$$\frac{1}{\sqrt{n^2}} \int dk_1 e^{-s[k_1^2 + \frac{(x-y)^2}{n^2}] - i\lambda x} = \frac{\pi}{s} e^{-\frac{\lambda^2}{4s} - i\lambda y} \quad (\text{F4})$$

we immediately verify that

$$I(y, \kappa, l^2, n^2) = \frac{1}{\sqrt{n^2}} \int dk_1 \int dx I[x, \kappa, l^2, k_1^2 + P_z^2(x-y)^2]. \quad (\text{F5})$$

A completely analogous derivation holds for the three-point function J , as well as for any scalar one-loop n -point function.

Appendix G: One-loop functions for the generalized Ioffe-time distributions and generalized pseudo-distributions

The Ioffe-time representation of the scalar one-loop function is obtained from Eq. (C8) as the Fourier transform

$$I^I(-\nu, \kappa, l^2, -z^2) = \int dy e^{i\nu y} I(y, \kappa, l^2, -z^2/\nu^2) \quad (\text{G1})$$

$$= \frac{N_c g_{\pi q}^2}{2\pi^2} \int_0^1 d\psi e^{i\nu\kappa\psi} K_0 \left(\sqrt{-z^2[M^2 + \psi(1-\psi)l^2]} \right).$$

In the evaluation we have used the covariant formula $n^2 = -z^2/\nu^2$, The corresponding pseudo-distribution is

$$I^P(x, \kappa, l^2, -z^2) = \int \frac{d\nu}{2\pi} e^{-i\nu x} I^I(\nu, \kappa, l^2, -z^2) = \frac{N_c g_{\pi q}^2}{2\pi^2} \times \int \frac{d\nu}{2\pi} \int_0^1 d\psi e^{-i\nu(x-\kappa\psi)} K_0 \left(\sqrt{-z^2[M^2 + \psi(1-\psi)l^2]} \right)$$

$$= \frac{N_c g_{\pi q}^2 \theta[x(\kappa-x)]}{2\pi^2 |\kappa|} K_0 \left(\sqrt{-z^2[M^2 + \frac{x}{\kappa}(1-\frac{x}{\kappa})l^2]} \right), \quad (\text{G2})$$

where in the last line we have applied the $\delta(x - \kappa\psi)$ function appearing in the second line. The symbol K_l denotes the modified Bessel function of the second kind.

Similarly, for the three-point function we find with Eq. (C13)

$$J^I(-\nu, \kappa, \kappa', l^2, l'^2, l \cdot l', -z^2) = \frac{N_c g_{\pi q}^2}{4\pi^2} \int_0^1 d\psi \int_0^1 d\tau \times \theta(1-\psi-\tau) e^{i\nu(\kappa\psi + \kappa'\tau)} \frac{\sqrt{-z^2}}{A} K_1(\sqrt{-z^2} A),$$

$$A = M^2 + \psi(1-\psi)l^2 + \tau(1-\tau)l'^2 - 2\psi\tau l \cdot l' \quad (\text{G3})$$

and

$$J^P(x, \kappa, \kappa', l^2, l'^2, l \cdot l', -z^2) = \frac{N_c g_{\pi q}^2}{4\pi^2} \int_0^1 d\psi \int_0^1 d\tau \times \\ \theta(1 - \psi - \tau) \delta(x - \kappa\psi - \kappa'\tau) \frac{\sqrt{-z^2}}{A} K_1(\sqrt{-z^2} A). \quad (\text{G4})$$

For our explicit kinematics, after doing the τ integration we get

$$J^P(x, \zeta, 1, t, m_\pi^2, -\frac{t}{2}, -z^2) = \frac{N_c g_{\pi q}^2}{4\pi^2} \times \\ \left[\theta[x(\zeta - x)] \int_0^{\frac{x}{\zeta}} d\psi + \theta[(1-x)(x - \zeta)] \int_0^{\frac{1-x}{1-\zeta}} d\psi \right] \times \\ \frac{\sqrt{-z^2}}{A} K_1(\sqrt{-z^2} A) \Big|_{\tau=x+\zeta\psi}, \quad (\text{G5})$$

with

$$A|_{\tau=x+\zeta\psi} = M^2 \\ -m_\pi^2(1 + \zeta\psi - x)(x - \zeta\psi) - t\psi(1 + \zeta\psi - x - \psi). \quad (\text{G6})$$

We also need (cf. Eq. (34)) the Fourier transforms of $J_1 \equiv yJ$, where

$$J_1^I(-\nu, \kappa, \kappa', l^2, l'^2, l \cdot l', -z^2) \\ = \int dy e^{i\nu y} y J = -i \frac{d}{d\nu} \int dy e^{i\nu y} J \\ = -i \frac{d}{d\nu} J^I(-\nu, \kappa, \kappa', l^2, l'^2, l \cdot l', -z^2), \quad (\text{G7})$$

and therefore

$$J_1^P(x, \kappa, \kappa', l^2, l'^2, l \cdot l', -z^2) \\ = x J^P(x, \kappa, \kappa', l^2, l'^2, l \cdot l', -z^2). \quad (\text{G8})$$

-
- [1] X. Ji, Phys. Rev. Lett. **110**, 262002 (2013), arXiv:1305.1539.
- [2] J.-W. Chen, S. D. Cohen, X. Ji, H.-W. Lin, and J.-H. Zhang, Nucl. Phys. B **911**, 246 (2016), arXiv:1603.06664 [hep-ph].
- [3] C. Alexandrou, K. Cichy, V. Drach, E. Garcia-Ramos, K. Hadjiyiannakou, K. Jansen, F. Steffens, and C. Wiese, Phys. Rev. **D92**, 014502 (2015), arXiv:1504.07455 [hep-lat].
- [4] C. Alexandrou, S. Bacchio, K. Cichy, M. Constantinou, K. Hadjiyiannakou, K. Jansen, G. Koutsou, A. Scapellato, and F. Steffens, EPJ Web Conf. **175**, 14008 (2018), arXiv:1710.06408 [hep-lat].
- [5] J.-H. Zhang, X. Ji, A. Schäfer, W. Wang, and S. Zhao, Phys. Rev. Lett. **122**, 142001 (2019), arXiv:1808.10824 [hep-ph].
- [6] T. Izubuchi, L. Jin, C. Kallidonis, N. Karthik, S. Mukherjee, P. Petreczky, C. Shugert, and S. Syritsyn, Phys. Rev. D **100**, 034516 (2019), arXiv:1905.06349 [hep-lat].
- [7] H.-W. Lin, J.-W. Chen, Z. Fan, J.-H. Zhang, and R. Zhang, Phys. Rev. D **103**, 014516 (2021), arXiv:2003.14128 [hep-lat].
- [8] X. Gao, L. Jin, C. Kallidonis, N. Karthik, S. Mukherjee, P. Petreczky, C. Shugert, S. Syritsyn, and Y. Zhao, Phys. Rev. D **102**, 094513 (2020), arXiv:2007.06590 [hep-lat].
- [9] L.-B. Chen, W. Wang, and R. Zhu, Phys. Rev. D **102**, 011503 (2020), arXiv:2005.13757 [hep-ph].
- [10] V. M. Braun, K. G. Chetyrkin, and B. A. Kniehl, JHEP **07**, 161 (2020), arXiv:2004.01043 [hep-ph].
- [11] X. Ji, Sci. China Phys. Mech. Astron. **57**, 1407 (2014), arXiv:1404.6680 [hep-ph].
- [12] J.-H. Zhang, J.-W. Chen, L. Jin, H.-W. Lin, A. Schäfer, and Y. Zhao, Phys. Rev. **D100**, 034505 (2019), arXiv:1804.01483 [hep-lat].
- [13] W. Wang, J.-H. Zhang, S. Zhao, and R. Zhu, Phys. Rev. D **100**, 074509 (2019), arXiv:1904.00978 [hep-ph].
- [14] X. Ji, Y.-S. Liu, Y. Liu, J.-H. Zhang, and Y. Zhao, Rev. Mod. Phys. **93**, 035005 (2021), arXiv:2004.03543 [hep-ph].
- [15] A. Radyushkin, Phys. Lett. B **767**, 314 (2017), arXiv:1612.05170.
- [16] A. V. Radyushkin, Phys. Rev. D **96**, 034025 (2017), arXiv:1705.01488.
- [17] K. Orginos, A. Radyushkin, J. Karpie, and S. Zafeiropoulos, Phys. Rev. D **96**, 094503 (2017), arXiv:1706.05373.
- [18] C. Monahan and K. Orginos, JHEP **03**, 116 (2017), arXiv:1612.01584 [hep-lat].
- [19] C. Monahan and K. Orginos, EPJ Web Conf. **175**, 06004 (2018), arXiv:1710.06466 [hep-lat].
- [20] A. V. Radyushkin, Phys. Lett. B **788**, 380 (2019), arXiv:1807.07509 [hep-ph].
- [21] J. Karpie, K. Orginos, and S. Zafeiropoulos, JHEP **11**, 178 (2018), arXiv:1807.10933 [hep-lat].
- [22] B. Joó, J. Karpie, K. Orginos, A. V. Radyushkin, D. G. Richards, R. S. Sufian, and S. Zafeiropoulos, Phys. Rev. D **100**, 114512 (2019), arXiv:1909.08517 [hep-lat].
- [23] B. Joó, J. Karpie, K. Orginos, A. Radyushkin, D. Richards, and S. Zafeiropoulos, JHEP **12**, 081 (2019), arXiv:1908.09771 [hep-lat].
- [24] J. Karpie, K. Orginos, A. Rothkopf, and S. Zafeiropoulos, JHEP **04**, 057 (2019), arXiv:1901.05408 [hep-lat].
- [25] L. Del Debbio, T. Giani, J. Karpie, K. Orginos, A. Radyushkin, and S. Zafeiropoulos, JHEP **02**, 138

- (2021), arXiv:2010.03996 [hep-ph].
- [26] B. Joó, J. Karpie, K. Orginos, A. V. Radyushkin, D. G. Richards, and S. Zafeiropoulos, (2020), arXiv:2004.01687 [hep-lat].
- [27] M. Bhat, K. Cichy, M. Constantinou, and A. Scapellato, Phys. Rev. D **103**, 034510 (2021), arXiv:2005.02102 [hep-lat].
- [28] Y.-Q. Ma and J.-W. Qiu, Phys. Rev. D **98**, 074021 (2018), arXiv:1404.6860 [hep-ph].
- [29] Y.-Q. Ma and J.-W. Qiu, Phys. Rev. Lett. **120**, 022003 (2018), arXiv:1709.03018 [hep-ph].
- [30] A. J. Chambers, R. Horsley, Y. Nakamura, H. Perlt, P. E. L. Rakow, G. Schierholz, A. Schiller, K. Somfleth, R. D. Young, and J. M. Zanotti, Phys. Rev. Lett. **118**, 242001 (2017), arXiv:1703.01153 [hep-lat].
- [31] G. Martinelli and C. T. Sachrajda, Phys. Lett. B **196**, 184 (1987).
- [32] A. Morelli, Nucl. Phys. B **392**, 518 (1993).
- [33] C. Best, M. Gockeler, R. Horsley, E.-M. Ilgenfritz, H. Perlt, P. E. Rakow, A. Schafer, G. Schierholz, A. Schiller, and S. Schramm, Phys. Rev. D **56**, 2743 (1997), arXiv:hep-lat/9703014.
- [34] W. Detmold, W. Melnitchouk, and A. W. Thomas, Phys. Rev. D **68**, 034025 (2003), arXiv:hep-lat/0303015.
- [35] X. Gao, A. D. Hanlon, N. Karthik, S. Mukherjee, P. Petreczky, P. Scior, S. Syritsyn, and Y. Zhao, (2022), arXiv:2206.04084 [hep-lat].
- [36] H.-W. Lin *et al.*, Prog. Part. Nucl. Phys. **100**, 107 (2018), arXiv:1711.07916 [hep-ph].
- [37] K. Cichy and M. Constantinou, Adv. High Energy Phys. **2019**, 3036904 (2019), arXiv:1811.07248 [hep-lat].
- [38] C. Monahan, PoS **LATTICE2018**, 018 (2018), arXiv:1811.00678 [hep-lat].
- [39] Y. Zhao, Int. J. Mod. Phys. A **33**, 1830033 (2019), arXiv:1812.07192 [hep-ph].
- [40] S. Amoroso *et al.*, (2022), arXiv:2203.13923 [hep-ph].
- [41] M. Burkardt and S. K. Seal, Phys. Rev. D **65**, 034501 (2002), arXiv:hep-ph/0102245.
- [42] M. Burkardt and S. Dalley, Prog. Part. Nucl. Phys **48**, 317 (2002), arXiv:hep-ph/0112007.
- [43] S. Dalley and B. van de Sande, Phys. Rev. D **67**, 114507 (2003), arXiv:hep-ph/0212086.
- [44] E. R. Arriola, Acta Phys. Polon. B **33**, 4443 (2002), arXiv:hep-ph/0210007.
- [45] W. Broniowski and E. R. Arriola, Phys. Lett. B **773**, 385 (2017), arXiv:1707.09588.
- [46] W. Broniowski and E. R. Arriola, Phys. Rev. D **97**, 034031 (2018), arXiv:1711.03377 [hep-ph].
- [47] V. Braun, P. Gornicki, and L. Mankiewicz, Phys. Rev. D **51**, 6036 (1995), arXiv:hep-ph/9410318.
- [48] W. Broniowski and E. Ruiz Arriola, PoS **Hadron2017**, 174 (2018), arXiv:1711.09355 [hep-ph].
- [49] A. Kock, Y. Liu, and I. Zahed, (2020), arXiv:2004.01595 [hep-ph].
- [50] L. Gamberg, Z.-B. Kang, I. Vitev, and H. Xing, Phys. Lett. **B743**, 112 (2015), arXiv:1412.3401 [hep-ph].
- [51] H.-D. Son, A. Tandogan, and M. V. Polyakov, Phys. Lett. B **808**, 135665 (2020), arXiv:1911.01955 [hep-ph].
- [52] H.-D. Son, (2022), arXiv:2203.17169 [hep-ph].
- [53] C. Tan and Z. Lu, (2022), arXiv:2206.06937 [hep-ph].
- [54] J. Badier *et al.* (NA3), Z. Phys. C **18**, 281 (1983).
- [55] J. S. Conway *et al.*, Phys. Rev. **D39**, 92 (1989).
- [56] S. Chekanov *et al.* (ZEUS), Nucl. Phys. B **637**, 3 (2002), arXiv:hep-ex/0205076.
- [57] F. D. Aaron *et al.* (H1), Eur. Phys. J. C **68**, 381 (2010), arXiv:1001.0532 [hep-ex].
- [58] P. C. Barry, C.-R. Ji, N. Sato, and W. Melnitchouk (Jefferson Lab Angular Momentum (JAM)), Phys. Rev. Lett. **127**, 232001 (2021), arXiv:2108.05822 [hep-ph].
- [59] B. Adams *et al.*, (2018), arXiv:1808.00848 [hep-ex].
- [60] R. Davidson and E. Ruiz Arriola, Phys. Lett. **B348**, 163 (1995).
- [61] R. M. Davidson and E. Ruiz Arriola, Acta Phys. Polon. **B33**, 1791 (2002), hep-ph/0110291.
- [62] A. E. Dorokhov and L. Tomio, Phys. Rev. **D62**, 014016 (2000).
- [63] I. V. Anikin, A. E. Dorokhov, and L. Tomio, Phys. Part. Nucl. **31**, 509 (2000).
- [64] S. Noguera and V. Vento, Eur. Phys. J. **A28**, 227 (2006), hep-ph/0505102.
- [65] T. Nguyen, A. Bashir, C. D. Roberts, and P. C. Tandy, Phys. Rev. C **83**, 062201 (2011), arXiv:1102.2448 [nucl-th].
- [66] L. Chang, C. Mezrag, H. Moutarde, C. D. Roberts, J. Rodríguez-Quintero, and P. C. Tandy, Phys. Lett. B **737**, 23 (2014), arXiv:1406.5450 [nucl-th].
- [67] J. Bartels and M. Loewe, Z. Phys. C **12**, 263 (1982).
- [68] B. Geyer, D. Robaschik, M. Bordag, and J. Horejsi, Z. Phys. C **26**, 591 (1985).
- [69] F. M. Dittes, D. Mueller, D. Robaschik, B. Geyer, and J. Horejsi, Phys. Lett. B **209**, 325 (1988).
- [70] X.-D. Ji, Phys. Rev. D **55**, 7114 (1997), arXiv:hep-ph/9609381.
- [71] A. V. Radyushkin, Phys. Rev. D **56**, 5524 (1997), arXiv:hep-ph/9704207.
- [72] M. Burkardt, Phys. Rev. D **62**, 071503 (2000), [Erratum: Phys.Rev.D 66, 119903 (2002)], arXiv:hep-ph/0005108.
- [73] M. Burkardt, Int. J. Mod. Phys. A **18**, 173 (2003), arXiv:hep-ph/0207047.
- [74] M. Burkardt and B. Pasquini, Eur. Phys. J. A **52**, 161 (2016), arXiv:1510.02567 [hep-ph].
- [75] B. Berthou *et al.*, Eur. Phys. J. C **78**, 478 (2018), arXiv:1512.06174 [hep-ph].
- [76] X. D. Ji, J. Phys. G **24**, 1181 (1998), arXiv:hep-ph/9807358.
- [77] A. V. Radyushkin, *Generalized parton distributions* ([hep-ph]) arXiv:hep-ph/0101225.
- [78] K. Goeke, M. V. Polyakov, and M. Vanderhaeghen, Prog. Part. Nucl. Phys **47**, 401 (2001), arXiv:hep-ph/0106012.
- [79] A. P. Bakulev, R. Ruskov, K. Goeke, and N. G. Stefanis, Phys. Rev. **D62**, 054018 (2000), hep-ph/0004111.
- [80] M. Diehl, Phys. Rept. **388**, 41 (2003), arXiv:hep-ph/0307382.
- [81] X. Ji, Ann. Rev. Nucl. Part. Sci. **54**, 413 (2004).
- [82] B. C. Tiburzi, *Light-front dynamics and generalized parton distributions*, Phd thesis (2004), arXiv:nucl-th/0407005.
- [83] A. V. Belitsky and A. V. Radyushkin, Phys. Rept. **418**, 1 (2005), hep-ph/0504030.
- [84] S. Boffi and B. Pasquini, (2007), arXiv:0711.2625 [hep-ph].
- [85] T. Feldmann, Eur. Phys. J. Special Topics **140**, 135 (2007).
- [86] D. Boer *et al.*, (2011), arXiv:1108.1713 [nucl-th].
- [87] M. Guidal, H. Moutarde, and M. Vanderhaeghen, Rept. Prog. Phys. **76**, 066202 (2013), arXiv:1303.6600 [hep-

- ph].
- [88] M. Praszalowicz and A. Rostworowski, in *Proceedings, 37th Rencontres de Moriond, 2002 QCD and high energy hadronic interactions : Les Arcs, Savoie, France, Mar 16-23, 2002*, edited by J. T. T. Van (2002) pp. 283 – 286, arXiv:hep-ph/0205177.
- [89] L. Theussl, S. Noguera, and V. Vento, *Eur. Phys. J.* **A20**, 483 (2004), nucl-th/0211036.
- [90] W. Broniowski, E. R. Arriola, and K. Golec-Biernat, *Phys. Rev. D* **77**, 034023 (2008), arXiv:0712.1012.
- [91] A. Courtoy, *Generalized Parton Distributions of Pions. Spin Structure of Hadrons*, Other thesis (2010), arXiv:1010.2974 [hep-ph].
- [92] A. E. Dorokhov, W. Broniowski, and E. R. Arriola, *Phys. Rev. D* **84**, 074015 (2011), arXiv:1107.5631.
- [93] J.-L. Zhang, M.-Y. Lai, H.-S. Zong, and J.-L. Ping, *Nucl. Phys. B* **966**, 115387 (2021).
- [94] L. Adhikari, C. Mondal, S. Nair, S. Xu, S. Jia, X. Zhao, and J. P. Vary (BLFQ), *Phys. Rev. D* **104**, 114019 (2021), arXiv:2110.05048 [hep-ph].
- [95] J.-L. Zhang, G.-Z. Kang, and J.-L. Ping, *Phys. Rev. D* **105**, 094015 (2022), arXiv:2204.14032 [hep-ph].
- [96] S. Dalley, *Phys. Lett.* **B570**, 191 (2003), hep-ph/0306121.
- [97] W. Broniowski and E. Ruiz Arriola, *Phys. Lett.* **B574**, 57 (2003), hep-ph/0307198.
- [98] J. D. Sullivan, *Phys. Rev. D* **5**, 1732 (1972).
- [99] A. C. Aguilar *et al.*, *Eur. Phys. J. A* **55**, 190 (2019), arXiv:1907.08218 [nucl-ex].
- [100] J. M. M. Chavez, V. Bertone, F. De Soto Borrero, M. Defurne, C. Mezrag, H. Moutarde, J. Rodríguez-Quintero, and J. Segovia, *Phys. Rev. D* **105**, 094012 (2022), arXiv:2110.06052 [hep-ph].
- [101] X. Ji, A. Schäfer, X. Xiong, and J.-H. Zhang, *Phys. Rev. D* **92**, 014039 (2015), arXiv:1506.00248 [hep-ph].
- [102] Y.-S. Liu, W. Wang, J. Xu, Q.-A. Zhang, J.-H. Zhang, S. Zhao, and Y. Zhao, *Phys. Rev. D* **100**, 034006 (2019), arXiv:1902.00307 [hep-ph].
- [103] A. V. Radyushkin, *Phys. Rev. D* **100**, 116011 (2019), arXiv:1909.08474 [hep-ph].
- [104] S. Bhattacharya, C. Cocuzza, and A. Metz, *Phys. Lett. B* **788**, 453 (2019), arXiv:1808.01437 [hep-ph].
- [105] Z.-L. Ma, J.-Q. Zhu, and Z. Lu, *Phys. Rev. D* **101**, 114005 (2020), arXiv:1912.12816 [hep-ph].
- [106] S. Bhattacharya, C. Cocuzza, and A. Metz, *Phys. Rev. D* **102**, 054021 (2020), arXiv:1903.05721 [hep-ph].
- [107] J.-W. Chen, H.-W. Lin, and J.-H. Zhang, *Nucl. Phys. B* **952**, 114940 (2020), arXiv:1904.12376 [hep-lat].
- [108] N. Karthik and R. S. Sufian, *Phys. Rev. D* **104**, 074506 (2021), arXiv:2106.03875 [hep-lat].
- [109] N. Karthik and R. Narayanan, *Phys. Rev. D* **106**, 014503 (2022), arXiv:2205.02252 [hep-lat].
- [110] J. Kwiecinski, *Acta Phys. Polon. B* **33**, 1809 (2002), arXiv:hep-ph/0203172.
- [111] A. Gawron and J. Kwiecinski, *Acta Phys. Polon. B* **34**, 133 (2003), arXiv:hep-ph/0207299.
- [112] A. Gawron, J. Kwiecinski, and W. Broniowski, *Phys. Rev. D* **68**, 054001 (2003), arXiv:hep-ph/0305219.
- [113] E. Ruiz Arriola and W. Broniowski, *Phys. Rev. D* **70**, 034012 (2004), hep-ph/0404008.
- [114] X. D. Ji, *Phys. Rev. Lett.* **78**, 610 (1997), arXiv:hep-ph/9603249.
- [115] A. V. Radyushkin, *Phys. Rev. D* **59**, 014030 (1999), hep-ph/9805342.
- [116] M. V. Polyakov and C. Weiss, *Phys. Rev. D* **60**, 114017 (1999), arXiv:hep-ph/9902451.
- [117] A. V. Efremov and A. V. Radyushkin, *Phys. Lett. B* **94**, 245 (1980).
- [118] G. P. Lepage and S. J. Brodsky, *Phys. Rev. D* **22**, 2157 (1980).
- [119] A. V. Radyushkin, *Phys. Lett. B* **380**, 417 (1996), arXiv:hep-ph/9604317.
- [120] W. Broniowski and E. Ruiz Arriola, *Phys. Rev. D* **78**, 094011 (2008), arXiv:0809.1744 [hep-ph].
- [121] J. F. Donoghue and H. Letutwyler, *Z. Phys.* **C52**, 343 (1991).
- [122] M. V. Polyakov and P. Schweitzer, *Int. J. Mod. Phys. A* **33**, 1830025 (2018), arXiv:1805.06596 [hep-ph].
- [123] A. V. Radyushkin, *Phys. Lett. B* **781**, 433 (2018), arXiv:1710.08813 [hep-ph].
- [124] A. V. Radyushkin, *Phys. Rev. D* **95**, 056020 (2017), arXiv:1701.02688.
- [125] M. Constantinou and H. Panagopoulos, *Phys. Rev. D* **96**, 054506 (2017), arXiv:1705.11193 [hep-lat].
- [126] H. Weigel, E. Ruiz Arriola, and L. P. Gamberg, *Nucl. Phys. B* **560**, 383 (1999), hep-ph/9905329.
- [127] E. Ruiz Arriola and W. Broniowski, *Phys. Rev. D* **66**, 094016 (2002), hep-ph/0207266.
- [128] W. Broniowski and E. Ruiz Arriola, *Phys. Rev. D* **101**, 014019 (2020), arXiv:1910.03707 [hep-ph].
- [129] W. Broniowski, E. Ruiz Arriola, and P. Sanchez-Puertas, *Phys. Rev. D* **106**, 036001 (2022), arXiv:2112.11049 [hep-ph].
- [130] W. Broniowski and E. R. Arriola, *Phys. Rev. D* **79**, 057501 (2009), arXiv:0901.3336 [hep-ph].
- [131] R. L. Workman (Particle Data Group), *PTEP* **2022**, 083C01 (2022).
- [132] W. Broniowski and E. Ruiz Arriola, *Phys. Lett. B*, 135803 (2020), arXiv:2006.03832 [hep-ph].